

Secrecy Outage Performance of Multi-antenna Wiretap Channels With Diversity Combinings Over Correlated Rayleigh Fading Channels

Jiangbo Si, *Member, IEEE*, Zan Li, *Senior Member, IEEE*,

Julian Cheng, *Senior Member, IEEE*, and Caijun Zhong, *Senior Member, IEEE*

Abstract

This paper presents a detailed secrecy outage performance analysis of correlated multi-antenna wiretap channels with three popular diversity combining schemes, namely maximal ratio combining, selection combining, and equal gain combining at the legitimate receiver. For single input multiple output wiretap channels, both exact and asymptotic expressions are derived for the secrecy outage probability (SOP) of these systems. The findings suggest that, compared with the scenario where all the channels are independent, correlation of the main channels alone increases the SOP by a factor of $1/\det(\mathbf{U})$, where $\det(\mathbf{U})$ is the determinant of correlation matrix \mathbf{U} . In contrast, in the high signal-to-noise ratio regime at the legitimate receiver, correlation between the main channels and the eavesdropper channels has a positive effect on SOP. Moreover, for multiple input and multiple output wiretap channels, the SOP of two transmit antenna selection (TAS) schemes are analyzed for the considered correlated channel model. The SOP relationship of the both TAS schemes is quantified by the secrecy array gain. Finally, numerical simulations are conducted to corroborate the analytical results.

Index Terms

Correlated Rayleigh fading, secrecy outage probability, transmit antenna selection.

Jiangbo Si and Zan Li are with the Integrated Service Networks Lab of Xidian University, Xi'an, China (e-mail: jbsi@xidian.edu.cn).

Julian Cheng is with the School of Engineering, The University of British Columbia, Kelowna, BC V1V 1V7, Canada (e-mail: julian.cheng@ubc.ca).

Caijun Zhong is with Information and Communication Engineering, Zhejiang University, Hangzhou 310027, China (e-mail: caijunzhong@zju.edu.cn).

I. INTRODUCTION

With the rapid penetration of wireless services into various aspects of the society, security has become an increasing critical concern. Responding to this concern, physical layer security (PLS) technique has emerged as a promising solution to provide secrecy communication, and has gained tremendous research attention in recent years. Since the pioneer work of Bloch *et al.* [1], who demonstrated that positive secrecy rate can be achieved regardless of the channel quality of the legitimate link, different approaches have been proposed in the literature to further enhance the secrecy performance of PLS. Among which, multiple antenna technology can provide the diversity gain and is of particular interest.

A plethora of works have investigated the impact of multiple antennas on the secrecy performance. For instance, the secrecy outage probability (SOP) of single-input multiple-output (SIMO) and multiple-input single-output (MISO) wiretap channels was studied in [2] and [3], respectively. Later on, the secrecy performance of multiple-input multiple-output (MIMO) wiretap channels was investigated in [4], [5]. In these prior works, it is commonly assumed that the channels are independent, which is a reasonable assumption when these multiple antennas are spaced sufficiently apart. In practice, due to space constraint, these multiple antennas can be correlated. In addition, the main channel and the eavesdropper channel can also be correlated when the eavesdropper is close to the legitimate receiver.

Therefore, understanding the impact of correlation on the secrecy performance of multi-antenna wiretap channels is of both theoretical and practical interests. By considering correlation at the multi-antenna legitimate receiver only, the effect of antenna correlation on the secrecy performance was investigated in [6], while the case with correlation at the multi-antenna eavesdropper only was examined in [7]. In [8], the impact of equal antenna correlation at both the multi-antenna legitimate receiver and eavesdropper on SOP was studied with maximum ratio combining (MRC). Later on, the extension to the arbitrary antenna correlation case was considered in [9] and [10]. Moreover, with antenna correlation at both the legitimate receiver and the eavesdropper, the SOP of transmit antenna selection (TAS) scheme was studied in [11].

In addition to the above works, which only focused on the antenna correlation, several works also investigated the secrecy performance when the main channel and eavesdropper channel are correlated. The secrecy capacity bounds for the correlated main and the eavesdropper channels were derived in [12]. The authors in [13] studied the the secrecy performance over correlated fading channels in the presence of a single-antenna eavesdropper. The secrecy performance over

correlated Nakagami-fading was recently presented in [14]. In [15], it was shown that the correlation between the legitimate receiver and eavesdropper channels can benefit secrecy performance in the high signal-to-noise ratio (SNR) regime. Similarly, in the cooperative relaying systems, it was shown that correlation between the relay-destination link and the relay-eavesdropper link is beneficial for the SOP [16]. Later on, the impacts of correlation on the SOP for different relay selection schemes were investigated in [17], where the authors showed that correlation can improve the SOP for full relay selection and degrade the SOP for the partial relay selection. For cognitive networks, the impact of correlation between the main channels and the eavesdropper channels on SOP was investigated in [18]. Also, secrecy key generation was proposed to take advantage of correlation between the main and eavesdropper channels [19].

However, one common limitation of the forementioned works is that they only considered the scenario with correlation between single antenna receiver and single antenna eavesdropper channels. In addition, the exact SOP gains due to correlation were not characterized. In modern communication system, communication terminals are likely equipped with multiple antennas. Therefore it is necessary to investigate the impact of correlation on SOP over multi-antenna wiretap channels. To the best of the authors' knowledge, the secrecy performance of general multi-antenna wiretap channels with arbitrary correlation between the main and eavesdropper's channels has not been well understood. Moreover, it is well known that the performance of diversity reception over independent channels is better than that over correlated channels [20]. However whether the secrecy performance over correlated channels is superior or inferior to that over independent channels is still an open question. Motivated by these, in this paper, we consider a more comprehensive system model with generalized correlation model. We systematically study the effect of correlation on the SOP for the SIMO wiretap channels, and the relationship of SOP over independent channels and correlated channels is quantified by simple and meaningful expressions. Furthermore, for a multi-antenna eavesdropper, we investigate the SOP of TAS schemes for the MIMO wiretap channels. Specifically, the main contributions of the paper are summarized as follows:

1. A joint probability density function (PDF) for a sum of correlated variables pertaining to our system model is first derived. Since the traditional correlation matrix eigenvalue decomposition technique [21] can not be used for SOP analysis in our scenario, we resort to the correlation channel model presented in [22]- [23] to establish the correlation between the main channels and the eavesdropper channels. All correlated channels are modeled as

a set of conditional independent channel gains. For this, the SOP can be derived by the method of moment generation function and conditional probability density function.

2. For three popular diversity combining schemes: MRC, selection combining (SC), and equal gain combining (EGC), simple asymptotic expressions are presented for the SOP of the considered system. The result indicates that the correlation does not change the secrecy diversity order. Moreover, the analytical findings suggest that, compared with the ideal case where all the channels are independent, antenna correlation of the main channels (CMC) increases the SOP by a factor of $1/\det(\mathbf{U})$ in the high SNR regime, where $\det(\mathbf{U})$ is the determinant of the main channels correlation matrix \mathbf{U} . In contrast, the correlation between the main and eavesdropper channels (CMEC) is beneficial for SOP. When the average SNR at the legitimate receiver is larger than that at the eavesdropper, the larger the correlation coefficient is, the more SOP gains can be obtained. Moreover, depending on the correlation coefficients, the combined effects due to correlation can either degrade or improve the SOP performance.
3. For correlated MIMO wiretap channels, two different types of TAS schemes are studied, depending on the availability of eavesdropper's channel state information (CSI). For both cases, N_E antennas are deployed at the eavesdropper, and the asymptotic SOP expressions of all three different diversity combining schemes are presented. The findings suggest that the considered TAS schemes achieve the same secrecy diversity order of MN_t , where N_t is the number of transmit antennas and M is the number of the receiver antennas. According to the secrecy array gain, the SOP gap of two TAS schemes is quantified by a closed-form expression and increases with N_t . Especially, when $N_E = 1$, compared with case of TAS with eavesdropper's CSI, the SOP of the TAS without eavesdropper's CSI deteriorates by a factor of $\frac{(MN_t)!}{(M!)^{N_t}}$.

The remainder of this paper is organized as follows. Section II describes the system model. In Section III, assuming a single antenna at the transmitter, the asymptotic expressions of SOP are derived. In Section IV, when multiple antennas are deployed at the transmitter and the eavesdropper, the asymptotic SOP expressions of TAS are derived with or without eavesdropper's CSI. Simulation results are presented in Section V. We conclude the paper in Section VI.

Notations- $\Pr(\cdot)$ denotes the probability of an event; $f_\beta(\cdot)$ is the PDF of random variable (RV) β ; $F_\beta(\cdot)$ is the cumulative distribution function (CDF) of RV β ; $I_0(\cdot)$ is the modified Bessel function of the first kind of order zero; $\phi_\beta(s)$ is the moment generation function (MGF)

of β ; $E(\cdot)$ is expected value of a RV; $\mathcal{L}^{-1}(\cdot)$ denotes the inverse Laplace transform; $\det(\cdot)$ is the determinant of a matrix; $\Gamma(\cdot)$ is the Gamma function; An $m \times m$ identity matrix is denoted by \mathbf{I}_m . ${}_1F_1(\alpha; \gamma; z)$ denotes the confluent hypergeometric function. ${}_2F_1(\alpha, \beta; \gamma; z)$ is the hypergeometric function. $E_n(\cdot)$ is the exponential-integral function. For a vector \mathbf{x} , \mathbf{x}^T denotes the transpose, and \mathbf{x}^H denotes the conjugate transpose.

II. SYSTEM MODEL

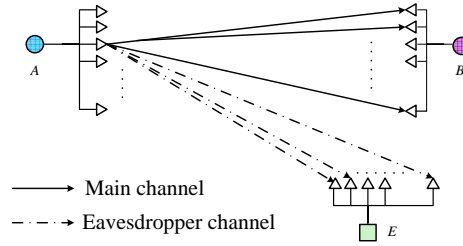


Fig. 1. System model of a multi-antenna secure communication systems

Consider a MIMO wiretap channel illustrated in Fig. 1, where the Alice or source node S equipped with N_t antennas aims to establish a secure communication link with the legitimate receiver B equipped with M antennas in the presence of eavesdropper E equipped with N_E antennas. All the channels are assumed to experience Rayleigh fading. When the signal is transmitted by the n -th antenna, the received signal at the legitimate receiver can be expressed as

$$\mathbf{y}_{s_n,B} = \sqrt{P_0} \mathbf{h}_{s_n,B} x + \mathbf{n}_B, n = 1, \dots, N_t \quad (1)$$

where x is the information symbol with unit power, P_0 is the source transmit power, and $\mathbf{h}_{s_n,B} = \{h_{s_n,b_1}, h_{s_n,b_2}, \dots, h_{s_n,b_M}\}^T$ is an $M \times 1$ channel vector between the n -th transmitter antenna and receiver. Also, h_{s_n,b_m} ($1 \leq m \leq M$) is a complex Gaussian RV with mean zero and variance $\frac{\sigma_{s,b}^2}{2}$. Finally, the $M \times 1$ vector \mathbf{n}_B denotes the additive white Gaussian noise (AWGN) at legitimate receiver satisfying $E(\mathbf{n}_B \mathbf{n}_B^H) = \mathbf{I}_M N_0$, where N_0 is the noise variance. Since the legitimate receiver has multiple antennas, diversity combining techniques can be employed to enhance the secrecy performance. Depending on the specific diversity combining schemes, the SNR at legitimate receiver, $\gamma_{s_n,B}$, takes different forms, which will be specified in the ensuing section. Similarly, the received signal at the eavesdroppers can be expressed as

$$\mathbf{y}_{s_n,E} = \sqrt{P_0} \mathbf{h}_{s_n,E} x + \mathbf{n}_E, n = 1, \dots, N_t \quad (2)$$

where $\mathbf{h}_{s_n,E} = \{h_{s_n,e_1}, h_{s_n,e_2}, \dots, h_{s_n,e_{N_E}}\}^T$ is the $N_E \times 1$ channel vector between the n -th transmitter antenna and the eavesdropper; h_{s_n,e_k} ($1 \leq k \leq N_E$) is an AWGN RV with mean zero and variance $\frac{\sigma_{s,e}^2}{2}$; \mathbf{n}_E is an AWGN RV vector at the eavesdropper satisfying $E(\mathbf{n}_E \mathbf{n}_E^H) = \mathbf{I}_{N_E} N_0$.

When multiple antennas are deployed at the legitimate receiver, due to the space constraint, the channels at multiple antennas are assumed to be correlated. In [22] and [24], the authors noted that a set of related complex Gaussian RVs can be obtained by linearly combining a set of independent Gaussian RVs. Then the correlated channel between the n -th antenna at the transmitter and the m -th antenna at the legitimate receiver, h_{s_n,b_m} , can be expressed as [23]

$$h_{s_n,b_m} = \sigma_{s_n,b_m} \left[\left(\sqrt{1 - \eta_m^2} X_{s_n,b_m} + \eta_m X_{n,0} \right) + i \left(\sqrt{1 - \eta_m^2} Y_{s_n,b_m} + \eta_m Y_{n,0} \right) \right], m = 1, \dots, M \quad (3)$$

where $i = \sqrt{-1}$, $-1 \leq \eta_m \leq 1$, and $X_{s_n,b_m}, Y_{s_n,b_m}, X_{n,0}, Y_{n,0}$ are independent Gaussian RVs with distribution $\mathcal{N}(0, 1/2)$. For any $m, m' \in \{1, \dots, M\}$, $E(X_{s_n,b_m} X_{s_n,b_{m'}}) = E(Y_{s_n,b_m} Y_{s_n,b_{m'}}) = \frac{1}{2} \delta_{m,m'}$, where $\delta_{u,v}$ is the Kronecker delta function, i.e., $\delta_{m,m'} = 1$ for $m = m'$ and $\delta_{m,m'} = 0$ for $m \neq m'$. Since the distance between the transmit antenna and the receive antenna is far greater than that between any two transmit antennas in practice, we assume all transmit antennas at the legitimate receiver have the same correlation matrix, which is defined as

$$\mathbf{U} = \begin{pmatrix} 1 & \rho_{1,2}^b & \cdots & \rho_{1,M}^b \\ \rho_{1,2}^b & 1 & \cdots & \rho_{2,M}^b \\ \vdots & \vdots & \ddots & \vdots \\ \rho_{1,M}^b & \rho_{2,M}^b & \cdots & 1 \end{pmatrix} \quad (4)$$

where the element $\rho_{m,m'}^b$ ($1 \leq m \leq M, 1 \leq m' \leq M, m \neq m'$) denotes the correlation coefficient between the m -th and m' -th receive antenna at the legitimate receiver, and it is calculated as

$$\rho_{m,m'}^b = \frac{E(h_{s_n,b_m} h_{s_n,b_{m'}}^*) - E(h_{s_n,b_m}) E(h_{s_n,b_{m'}}^*)}{\sqrt{E(|h_{s_n,b_m}|^2) E(|h_{s_n,b_{m'}}|^2)}} = \eta_m \eta_{m'} \quad (5)$$

When the eavesdropper is close to the legitimate receiver, the signal received at the legitimate receiver can be correlated with signal at the eavesdropper. Also, when the eavesdropper lies in the radio wave path of legitimated signal and the eavesdropper is less than 70-80 wavelengths from the legitimate receiver (see [12] and reference therein), the received signal at the legitimate

receiver and the eavesdropper can be correlated. Thus, we can model the eavesdropper's channel as

$$h_{s_n, e_k} = \sigma_{s,e} \left[\left(\sqrt{1 - \lambda_k^2} X_{s_n, e_k} + \lambda_k X_{n,0} \right) + i \left(\sqrt{1 - \lambda_k^2} Y_{s_n, e_k} + \lambda_k Y_{n,0} \right) \right], k = 1, \dots, N_E \quad (6)$$

where $-1 \leq \lambda_k \leq 1$; X_{s_n, e_k} and Y_{s_n, e_k} are independent Gaussian RVs with distribution $\mathcal{N}(0, 1/2)$. In this paper, for analytical convenience, we assume the eavesdropper channels are equally correlated, $\lambda_k = \lambda_e$. Thus, similar to (5), the correlation coefficient between h_{s_n, e_ϑ} and $h_{s_n, e_{\vartheta'}}$ ($1 \leq \vartheta \leq N_E$) is

$$\rho_{\vartheta, \vartheta'}^e = \lambda_e^2. \quad (7)$$

As an important contribution of this work, we establish correlation between the main channels and the eavesdropper channels via the common variables $X_{n,0}$ and $Y_{n,0}$ in both (3) and (6). As a result, the correlation coefficient between h_{s_n, b_m} and h_{s_n, e_ϑ} can be concisely expressed as

$$\rho_{m, \vartheta}^{b,e} = \eta_m \lambda_e. \quad (8)$$

To evaluate the secrecy performance for more general scenarios, classical information-theoretic methods are often deployed [2]- [18]. For the information-theoretic secrecy evaluation, the SOP, non-zero capacity rate, and average secrecy capacity are three popular and common metrics¹ [1]. Since we consider the case that the eavesdropper's CSI is unavailable, and the probability of non-zero secrecy rate can be easily obtained by the special case of SOP, we will employ the SOP to evaluate the secrecy performance. When the n -th transmit antenna is selected, the secrecy capacity is expressed as

$$C_{s_n} = \begin{cases} \log_2(1 + \gamma_{s_n, B}) - \log_2(1 + \gamma_{s_n, E}), & \gamma_{s_n, B} \geq \gamma_{s_n, E} \\ 0, & \gamma_{s_n, B} < \gamma_{s_n, E} \end{cases} \quad (9)$$

where $\gamma_{s_n, B}$ and $\gamma_{s_n, E}$ denote the SNR at the legitimate receiver and eavesdropper, respectively. The SOP is defined as the probability that C_{s_n} is less than a predetermined secrecy rate R_s . It can be written as [26], [27]

$$\begin{aligned} P_{out}(R_s) &= \Pr(C_{s_n} < R_s) \\ &= \Pr(\gamma_{s_n, B} < 2^{R_s} (1 + \gamma_{s_n, E}) - 1). \end{aligned} \quad (10)$$

In the remainder of the paper, the definition in (10) is used to evaluate the secrecy performance.

¹It is worth noting that several new secrecy performance metrics have recently been proposed by taking into account of the eavesdropper's decodability of confidential messages [25].

III. SOP WITH SINGLE ANTENNA AT THE TRANSMITTER AND THE EAVESDROPPER

In this section, we analyze the SOP of a SIMO system, which may correspond to an uplink of a cellular network, where the base station is equipped with multiple antennas, and the terminal is often equipped with single antenna due to size and cost constraint. It is valuable to evaluate the SOP performance of the SIMO system with a single-antenna eavesdropper, per the discussions in [13]- [17]. Moreover, the case of multi-antenna eavesdropper will be considered in Section IV. This section also forms the basis of analysis for TAS with or without eavesdropper's CSI in Section IV.

In particular, we consider three different diversity combining schemes adopted at the legitimate receiver, namely, MRC, SC and EGC. Each combining scheme has its advantage and disadvantage. MRC requires accurate instantaneous CSI and can achieve the best performance. SC compares all branches instantaneous CSI and has a simple structure. However, the performance of SC is much lower than that of MRC. To compromise the system performance and complexity, EGC is a suitable choice. For the correlated SIMO wiretap channels, we consider these three popular diversity combining schemes at the legitimate receiver. Next, the impacts of correlation on SOP for three combining schemes are analytically quantified in detail.

A. MRC at the Legitimate Receiver

When MRC is adopted at the legitimate receiver, the SNR is given by

$$\gamma_{s_n,B}^{MRC} = \gamma_{s_n,b_1} + \gamma_{s_n,b_2} + \cdots + \gamma_{s_n,b_M} \quad (11)$$

where $\gamma_{s_n,b_m} = \frac{P_0 |h_{s_n,b_m}|^2}{N_0}$ ($1 \leq m \leq M$) is exponentially distributed with mean $\bar{\gamma}_{s_n,b_m} = \frac{P_0 \sigma_{s_n,b_m}^2}{N_0}$. Since the antennas are co-located, it is reasonable to assume that the main channels at the legitimate receiver have the same average SNR $\bar{\gamma}_{s_n,b_m} = \bar{\gamma}_B$.

1) *Exact SOP*: When the main channels and the eavesdropper channel are correlated. The SNR at the destination has been presented in (11). Since $\gamma_{s_n,B}^{MRC}$ and $\gamma_{s_n,E}$ are correlated, and all the variables in (11) and $\gamma_{s_n,E}$ are correlated, it is challenging to derive the exact SOP for arbitrarily correlated fading channels. We only discuss the exact SOP for equally correlated case. We can resort to the conditional CDF to derive the exact SOP. We assume $T = X_{n,0}^2 + Y_{n,0}^2$, $X_{n,0} = x_0$, and $Y_{n,0} = y_0$. If the main channels are equally correlated, i. e., $\rho_{m,m'}^b = \rho$, conditioned on

$x_0^2 + y_0^2 = t$, $\gamma_{s_n, B}^{MRC}$ has a noncentral chi-square distribution $\chi_{2M} \left(\sqrt{M\bar{\gamma}_B\rho^2 t}, \frac{\bar{\gamma}_B(1-\rho^2)}{2} \right)$, and the conditional CDF of $\gamma_{s_n, B}^{MRC}$ is given by

$$F_{\gamma_{s_n, B}^{MRC}|T}(x|t) = 1 - Q_M \left(\sqrt{\frac{2M\rho^2 t}{1-\rho^2}}, \sqrt{\frac{2x}{\bar{\gamma}_B(1-\rho^2)}} \right) \quad (12)$$

where $Q_M(\cdot, \cdot)$ denotes the M -th order Marcum Q -function, and it is defined as [22]

$$Q_M(a, b) = \int_b^\infty x \left(\frac{x}{a} \right)^{M-1} \exp \left(- \left(\frac{x^2 + a^2}{2} \right) \right) I_{M-1}(ax) dx. \quad (13)$$

Similarly, conditioned on $x_0^2 + y_0^2 = t$, $\gamma_{s_n, E}$ has a noncentral chi-square distribution $\chi_2 \left(\sqrt{\bar{\gamma}_E\lambda_e^2 t}, \frac{\bar{\gamma}_E(1-\lambda_e^2)}{2} \right)$, and the conditional CDF of $\gamma_{s_n, E}$ is given by

$$F_{\gamma_{s_n, E}|T}(y|t) = 1 - Q_1 \left(\sqrt{\frac{2\lambda_e^2 t}{1-\lambda_e^2}}, \sqrt{\frac{2y}{\bar{\gamma}_E(1-\lambda_e^2)}} \right) \quad (14)$$

where $Q_1(\cdot, \cdot)$ denotes the first-order Marcum Q -function. Differentiating (14) with respect to y , the conditional PDF of $\gamma_{s_n, E}$ is derived as

$$f_{\gamma_{s_n, E}|T}(y|t) = \frac{\exp \left(-\frac{\lambda_e^2 t}{1-\lambda_e^2} \right)}{\bar{\gamma}_E(1-\lambda_e^2)} \exp \left(-\frac{y}{\bar{\gamma}_E(1-\lambda_e^2)} \right) I_0 \left(2\sqrt{\frac{\lambda_e^2 t y}{\bar{\gamma}_E(1-\lambda_e^2)^2}} \right). \quad (15)$$

According to (10), (12), and (15), the SOP of MRC is given by

$$\begin{aligned} P_{out_MRC}(R_s) &= \int_0^\infty \exp(-t) \Pr \left(\gamma_{s_n, B}^{MRC} \leq 2^{R_s} (\gamma_{s_n, E} + 1) - 1 | t \right) dt \\ &= \int_0^\infty e^{-t} dt \int_0^\infty \left(1 - Q_M \left(\sqrt{\frac{2M\rho^2 t}{1-\rho^2}}, \sqrt{\frac{2(2^{R_s}(y+1)-1)}{\bar{\gamma}_B(1-\rho^2)}} \right) \right) \\ &\quad \times \frac{\exp \left(-\frac{\lambda_e^2 t}{1-\lambda_e^2} \right)}{\bar{\gamma}_E(1-\lambda_e^2)} \exp \left(-\frac{y}{\bar{\gamma}_E(1-\lambda_e^2)} \right) I_0 \left(2\sqrt{\frac{\lambda_e^2 t y}{\bar{\gamma}_E(1-\lambda_e^2)^2}} \right) dy. \end{aligned} \quad (16)$$

By using the function MARCUMQ provided in Matlab, the exact SOP of MRC can be obtained.

2) *Asymptotic SOP*: If the correlation coefficients are arbitrary, it is challenging to obtain the conditional CDF or PDF of $\gamma_{s_n, B}^{MRC}$ and the direct method to derive the SOP is intractable. We resort to the conditional MGF to obtain the asymptotic SOP with arbitrary correlation at the legitimate receiver. As $\bar{\gamma}_B \rightarrow \infty$, it corresponds to the scenario where the main channels have good quality while the eavesdropper's channel is severely blocked due to severe shadowing. The

asymptotic conditional PDF of $\gamma_{s_n,B}^{MRC}$ is derived in Appendix A. According to (15) and (69), as $\bar{\gamma}_B \rightarrow \infty$, we can obtain the asymptotic SOP of MRC as

$$\begin{aligned} P_{out_MRC}^{\bar{\gamma}_B \rightarrow \infty}(R_s) &= \int_0^\infty \exp(-t) dt \int_0^\infty (\gamma_{s_n,B}^{MRC} \leq 2^{R_s} (1+y) - 1) f_{\gamma_{s_n,E}}(y|t) dy \\ &= \frac{\bar{\gamma}_E^M}{\det(\mathbf{U}) \bar{\gamma}_B^M} \sum_{k=0}^M \frac{1}{(M-k)!} \left(\frac{1 + \sum_{m=1}^M \frac{\eta_m^2 (1-\lambda_e^2)}{1-\eta_m^2}}{1 + \sum_{m=1}^M \frac{\eta_m^2}{1-\eta_m^2}} \right)^k \left(\frac{2^{R_s} - 1}{\bar{\gamma}_E} \right)^{M-k} (2^{R_s})^k + o\left(\frac{1}{\bar{\gamma}_B^M}\right) \end{aligned} \quad (17)$$

where in obtaining the last equality the following integral identity

$$\int_0^\infty \exp(-\mu x) I_0(2\sqrt{vx}) dx = \frac{1}{\mu} \exp\left(\frac{v}{\mu}\right) \quad (18)$$

is used [28]. In (17), $o(\cdot)$ denotes higher order terms; $\det(\mathbf{U})$ is the determinant of matrix \mathbf{U} , and it is given by [29]

$$\det(\mathbf{U}) = \prod_{m=1}^M (1 - \eta_m^2) \left(1 + \sum_{m=1}^M \frac{\eta_m^2}{1 - \eta_m^2} \right). \quad (19)$$

It can be seen from (17) that the diversity order is M . In addition, if $\bar{\gamma}_E \gg 1$, eq. (17) can be further simplified as

$$P_{out_MRC}(R_s) \simeq \frac{1}{\det(\mathbf{U})} \left(\frac{2^{R_s} \bar{\gamma}_E}{\bar{\gamma}_B} \right)^M \left(\frac{1 + \sum_{m=1}^M \frac{\eta_m^2 (1-\lambda_e^2)}{1-\eta_m^2}}{1 + \sum_{m=1}^M \frac{\eta_m^2}{1-\eta_m^2}} \right)^M. \quad (20)$$

Since the asymptotic SOP with $\bar{\gamma}_E \gg 1$ can be easily obtained by the asymptotic SOP, in the remainder of the paper, unless otherwise stated, we will not derive the asymptotic SOPs with $\bar{\gamma}_E \gg 1$.

B. SC at the Legitimate Receiver

When the SC is applied, the SNR at the multi-antennas legitimate receiver is given by

$$\gamma_{s_n,B}^{SC} = \max(\gamma_{s_n,b_1}, \gamma_{s_n,b_2}, \dots, \gamma_{s_n,b_M}). \quad (21)$$

1) *Exact SOP*: When SC is applied at the legitimate receiver, the SNR at the legitimate receiver has been given in (21). Since the main and eavesdropper's channels are correlated, similar to the case of MRC, the conditional CDF approach is used. For fixed $X_{n,0} = x_0$, $Y_{n,0} = y_0$, the conditional h_{s_n,b_m} is complex Gaussian distributed with mean $\sqrt{\bar{\gamma}_B \eta_m^2} (x_0 + iy_0)$ and variance

$\frac{\bar{\gamma}_B(1-\eta_m^2)}{2} \cdot |h_{s_n,b_m}|^2$ obeys a noncentral chi-square distribution $\chi_2 \left(\sqrt{\bar{\gamma}_B \eta_m^2 (x_0^2 + y_0^2)}, \frac{\bar{\gamma}_B(1-\eta_m^2)}{2} \right)$. Assuming $T = X_{n,0}^2 + Y_{n,0}^2$ with $x_0^2 + y_0^2 = t$, the conditional CDF of γ_{s_n,b_m} can be obtained as

$$\begin{aligned} F_{\gamma_{s_n,b_m}|T}(x|t) &= \Pr(\gamma_{s_n,b_m} \leq x|t) \\ &= 1 - Q_1 \left(\sqrt{\frac{2\eta_m^2 t}{1-\eta_m^2}}, \sqrt{\frac{2x}{\bar{\gamma}_B(1-\eta_m^2)}} \right). \end{aligned} \quad (22)$$

According to (21) and (65), the conditional CDF of $\gamma_{s_n,B}^{SC}$ is expressed as

$$F_{\gamma_{s_n,B}^{SC}|T}(x|t) = \prod_{m=1}^M \left(1 - Q_1 \left(\sqrt{\frac{2\eta_m^2 t}{1-\eta_m^2}}, \sqrt{\frac{2x}{\bar{\gamma}_B(1-\eta_m^2)}} \right) \right). \quad (23)$$

The SOP of SC is given by

$$\begin{aligned} P_{out_SC}(R_s) &= \int_0^\infty e^{-t} \Pr(\gamma_{s_n,B}^{SC} \leq (2^{R_s}(\gamma_{s_n,E} + 1) - 1) | t) dt \\ &= \int_0^\infty e^{-t} dt \int_0^\infty \prod_{m=1}^M Q_1 \left(\sqrt{\frac{2\eta_m^2 t}{1-\eta_m^2}}, \sqrt{\frac{2(2^{R_s}(y+1)-1)}{\bar{\gamma}_B(1-\eta_m^2)}} \right) f_{\gamma_{s_n,E}}(y|t) dy \\ &= \int_0^\infty \prod_{m=1}^M Q_1 \left(\sqrt{\frac{2\eta_m^2 t}{1-\eta_m^2}}, \sqrt{\frac{2(2^{R_s}(y+1)-1)}{\bar{\gamma}_B(1-\eta_m^2)}} \right) \exp\left(-\frac{y}{\bar{\gamma}_E(1-\lambda_e^2)}\right) I_0 \left(\sqrt{\frac{2\lambda_e^2 t}{1-\lambda_e^2}} y \right) dy \\ &\quad \times \int_0^\infty \frac{\exp\left(-\frac{t}{1-\lambda_e^2}\right)}{\bar{\gamma}_B(1-\lambda_e^2)} dt. \end{aligned} \quad (24)$$

2) *Asymptotic SOP:* As $\beta \rightarrow 0^+$, $Q_M(\alpha, \beta)$ can be approximated as [30]

$$Q_M(\alpha, \beta) \approx 1 - \frac{\beta^{2M}}{2^M M!} \exp\left(-\frac{\alpha^2}{2}\right). \quad (25)$$

As $\bar{\gamma}_B \rightarrow \infty$, substituting (25) into (24), the asymptotic SOP is derived as

$$P_{out_SC}^{\bar{\gamma}_B \rightarrow \infty}(R_s) = \frac{M! \bar{\gamma}_E^M}{\det(\mathbf{U}) \bar{\gamma}_B^M} \sum_{k=0}^M \frac{(2^{R_s})^k}{(M-k)!} \left(\frac{1 + \sum_{k=1}^M \frac{\eta_m^2(1-\lambda_e^2)}{1-\eta_m^2}}{1 + \sum_{m=1}^M \frac{\eta_m^2}{1-\eta_m^2}} \right)^k \left(\frac{2^{R_s} - 1}{\bar{\gamma}_E} \right)^{M-k} + o\left(\frac{1}{\bar{\gamma}_B^M}\right). \quad (26)$$

It can be seen from (26) that the diversity order is still M .

C. EGC at the Legitimate Receiver

When the EGC is applied, the received signals are first co-phased and then summed to form the resultant output. The SNR at the multi-antenna legitimate receiver is given by

$$\gamma_{s_n,B}^{EGC} = \frac{P_0 \left(\sum_{m=1}^M |h_{s_n,b_m}| \right)^2}{MN_0} = \frac{\left(\sum_{m=1}^M \sqrt{\gamma_{s_n,b_m}} \right)^2}{M}. \quad (27)$$

Since $\gamma_{s_n,B}^{EGC}$ is correlated with γ_E , it is challenging to derive $\gamma_{s_n,B}^{EGC}$ directly. Different from the case of MRC, we derive the conditional PDF of $\gamma_{s_n,B}^{EGC}$ in Appendix B. Then according to (10), (15), and (76), the asymptotic SOP of EGC is derived as

$$\begin{aligned}
P_{out_EGC}^C(R_s) &= \Pr\left(\gamma_{s_n,B}^{EGC} \leq \left(2^{R_s}(\gamma_{s_n,E} + 1) - 1\right)\right) \\
&= \int_0^\infty e^{-t} dt \int_0^\infty f_{\gamma_{s_n,E}|T}(y|t) \int_0^{2^{R_s}(y+1)-1} f_{\gamma_{s_n,B}|T}(x|t) dx dy \\
&= \frac{M!(2M)^M \bar{\gamma}_E^M}{(2M)! \det(\mathbf{U}) \bar{\gamma}_B^M} \sum_{k=0}^M \frac{1}{(M-k)!} \left(\frac{1 + \sum_{m=1}^M \frac{\eta_m^2(1-\lambda_e^2)}{1-\eta_m^2}}{1 + \sum_{m=1}^M \frac{\eta_m^2}{1-\eta_m^2}} \right)^k \left(\frac{2^{R_s} - 1}{\bar{\gamma}_E} \right)^{M-k} (2^{R_s})^k + o\left(\frac{1}{\bar{\gamma}_B^M}\right).
\end{aligned} \tag{28}$$

It can be observed from (28) that the diversity order is still M .

D. Special Case of $\lambda_e = 0$

As $\lambda_e = 0$, the main channels and the eavesdropper channel are independent. Eqs. (17), (26), and (28) are, respectively, simplified to

$$P_{out_MRC}^C(R_s) = \frac{\bar{\gamma}_E^M}{\bar{\gamma}_B^M \det(\mathbf{U})} \sum_{k=0}^M \frac{1}{(M-k)!} \left(\frac{2^{R_s} - 1}{\bar{\gamma}_E} \right)^{M-k} (2^{R_s})^k + o\left(\frac{1}{\bar{\gamma}_B^M}\right) \tag{29}$$

$$P_{out_SC}^C(R_s) = \frac{M! \bar{\gamma}_E^M}{\bar{\gamma}_B^M \det(\mathbf{U})} \sum_{k=0}^M \frac{1}{(M-k)!} \left(\frac{2^{R_s} - 1}{\bar{\gamma}_E} \right)^{M-k} (2^{R_s})^k + o\left(\frac{1}{\bar{\gamma}_B^M}\right) \tag{30}$$

$$P_{out_EGC}^C(R_s) = \frac{M!(2M)^M \bar{\gamma}_E^M}{(2M)! \det(\mathbf{U}) \bar{\gamma}_B^M} \sum_{k=0}^M \frac{1}{(M-k)!} \left(\frac{2^{R_s} - 1}{\bar{\gamma}_E} \right)^{M-k} (2^{R_s})^k + o\left(\frac{1}{\bar{\gamma}_B^M}\right). \tag{31}$$

a) $\eta_m^2 = 1$: When $\eta_m^2 = 1$ ($1 \leq m \leq M$) or $\det(\mathbf{U}) = 0$, the main channels are completely correlated. In this case, the SOP of different combining schemes is given by

$$P_{out}^C(R_s) = \frac{\bar{\gamma}_E}{\varepsilon \bar{\gamma}_B} \left(2^{R_s} + \frac{2^{R_s} - 1}{\bar{\gamma}_E} \right). \tag{32}$$

In (32), as MRC and EGC are deployed at the legitimate receiver, $\varepsilon = M$. As SC is deployed, $\varepsilon = 1$. It is obvious from (32), the secrecy diversity order decreases to unity when the main channels are completely correlated.

b) $\eta_m = 0$: When $\lambda_e = 0$, and $\eta_m = 0$, namely $\det(\mathbf{U}) = 1$, all the channels are independent. Eqs. (17), (26), and (28) are, respectively, simplified as

$$P_{\bar{\gamma}_B \rightarrow \infty}^{I, \text{MRC}}(R_s) = \frac{\bar{\gamma}_E^M}{\bar{\gamma}_B^M} \sum_{k=0}^M \frac{1}{(M-k)!} \left(\frac{2^{R_s} - 1}{\bar{\gamma}_E} \right)^{M-k} (2^{R_s})^k + o\left(\frac{1}{\bar{\gamma}_B^M}\right) \quad (33)$$

$$P_{\bar{\gamma}_B \rightarrow \infty}^{I, \text{SC}}(R_s) = \frac{M! \bar{\gamma}_E^M}{\bar{\gamma}_B^M} \sum_{k=0}^M \frac{1}{(M-k)!} \left(\frac{2^{R_s} - 1}{\bar{\gamma}_E} \right)^{M-k} (2^{R_s})^k + o\left(\frac{1}{\bar{\gamma}_B^M}\right) \quad (34)$$

$$P_{\bar{\gamma}_B \rightarrow \infty}^{I, \text{EGC}}(R_s) = \frac{M! (2M)^M \bar{\gamma}_E^M}{(2M)! \bar{\gamma}_B^M} \sum_{k=0}^M \frac{1}{(M-k)!} \left(\frac{2^{R_s} - 1}{\bar{\gamma}_E} \right)^{M-k} (2^{R_s})^k + o\left(\frac{1}{\bar{\gamma}_B^M}\right). \quad (35)$$

Remark 1: Comparing the case of having only antenna correlation at the legitimate receiver with the case where all the channels are independent, we reveal that antenna correlation at the legitimate receiver increases the SOP by a factor of $1/\det(\mathbf{U})$. Since $\det(\mathbf{U}) \leq 1$ [31], [32], antenna correlation at the legitimate receiver deteriorates the SOP. The higher antenna correlation becomes, the worse SOP is obtained. Moreover, it can be seen that regardless which diversity reception is deployed at the legitimate receiver, CMC does not change the secrecy diversity order M . In addition, it can be seen that as $\bar{\gamma}_B \rightarrow \infty$, no matter whether the main channels are correlated or not, the SOP of SC is $M!$ times that of MRC, and the SOP of EGC is $\frac{M!(2M)^M}{(2M)!}$ times that of MRC.

E. Comparison of CMEC With CMC

Comparing (17), (26), (28) with (29), (30), (31), as $\bar{\gamma}_E \gg 1$, for the three combining schemes we can find

$$\lim_{\bar{\gamma}_B \rightarrow \infty} \frac{P_{out}(R_s)}{P_{out}^C(R_s)} = \left(\frac{1 + \sum_{k=1}^M \frac{\eta_m^2 (1 - \lambda_e^2)}{1 - \eta_m^2}}{1 + \sum_{k=1}^M \frac{\eta_m^2}{1 - \eta_m^2}} \right)^M. \quad (36)$$

Because $\frac{1 + \sum_{m=1}^M \frac{\eta_m^2 (1 - \lambda_e^2)}{1 - \eta_m^2}}{1 + \sum_{m=1}^M \frac{\eta_m^2}{1 - \eta_m^2}} \leq 1$, $P_{out_MRC}(R_s) \leq P_{out_MRC}^C(R_s)$, $P_{out_SC}(R_s) \leq P_{out_SC}^C(R_s)$, and $P_{out_EGC}(R_s) \leq P_{out_EGC}^C(R_s)$.

Remark 2: we can conclude that in the high SNR regime at the legitimate receiver, the correlation between the main channels and the eavesdropper channel improves the SOP performance. While similar conclusion was made for the single-antenna main channel and the single-antenna

eavesdropper channel [15]. We emphasize that the same conclusion can be made for multi-antenna main channels here, as well as for multi-antenna eavesdropper channels in Section IV. This phenomenon can be intuitively understood by analyzing the SOP under the extreme case that the main and eavesdropper channels are fully correlated, where the instantaneous SNR at the legitimate receiver is always larger than that at the eavesdropper, and the best SOP performance can be obtained. Note that (36) is obtained when $\bar{\gamma}_B$ approaches infinity. Hence, our statement holds under the condition that the average SNR $\bar{\gamma}_B$ at the legitimate receiver is much larger than the average SNR at the eavesdropper $\bar{\gamma}_E$.

F. Comparison of CMEC with Independent of All The Channels

Comparing (17) with (33), (26) with (34), and (28) with (35), as $\bar{\gamma}_E \gg 1$, for the three combining schemes, the relationship between the SOP under the case when all the channels are correlated and the SOP under the case when all the channels are independent is given by

$$\lim_{\bar{\gamma}_B \rightarrow \infty} \frac{P_{out}(R_s)}{P_{out}^I(R_s)} = \frac{1}{\det(\mathbf{U})} \left(\frac{1 + \sum_{m=1}^M \frac{\eta_m^2 (1 - \lambda_e^2)}{1 - \eta_m^2}}{1 + \sum_{k=1}^M \frac{\eta_m^2}{1 - \eta_m^2}} \right)^M. \quad (37)$$

Remark 3: Setting $P_{out}^I(R_s)$ as the reference, it can be easily concluded from (37) that, in the high SNR regime, the SOP decreases with λ_e^2 . Moreover, note that in (37) the first part $\frac{1}{\det(\mathbf{U})} \geq 1$, and the second part $\left(\frac{1 + \sum_{m=1}^M \frac{\eta_m^2 (1 - \lambda_e^2)}{1 - \eta_m^2}}{1 + \sum_{k=1}^M \frac{\eta_m^2}{1 - \eta_m^2}} \right)^M \leq 1$. This leads to $\frac{P_{out}(R_s)}{P_{out}^I(R_s)} \leq 1$ when λ_e^2 is large and the main channels are slightly correlated. In other words, the combined effects of the antenna correlation at the legitimate receiver (η_m) and the correlation between the main channels and eavesdropper channel (λ_e) can either degrade or improve the SOP performance.

G. Lower and Upper SOP Bounds with Correlation Between The Main and Eavesdropper Channels

In Remark 2, we have known the SOP decreases with λ_e^2 , when the main and eavesdropper channels are correlated. Then with fixed antenna correlation matrix \mathbf{U} and the fixed average

channel gains $\bar{\gamma}_B$ and $\bar{\gamma}_E$, the lower bound of SOP can be obtained by letting $\lambda_e^2 = 1$. For the special case of $\lambda_e^2 = 1$, as $\bar{\gamma}_B \rightarrow \infty$, the asymptotic SOP of MRC is recalculated as

$$\begin{aligned} P_{out_MRC} &= \Pr \left(\gamma_{s_n, B}^{mrc} \leq 2^{R_s} (\gamma_E + 1) - 1 \right) = \int_0^\infty e^{-t} \int_0^{2^{R_s}(\bar{\gamma}_E t + 1) - 1} f_{\gamma_{B_mrc}}(x) dx \\ &= \frac{\bar{\gamma}_E^M}{\bar{\gamma}_B^M \det(\mathbf{U})} \sum_{k=0}^M \frac{1}{\left(1 + \sum_{m=1}^M \frac{\eta_m^2}{1 - \eta_m^2}\right)^k} \frac{1}{(M-k)!} \left(\frac{2^{R_s} - 1}{\bar{\gamma}_E}\right)^{M-k} 2^{R_s k} + o\left(\frac{1}{\bar{\gamma}_B^M}\right). \end{aligned} \quad (38)$$

Similarly, the asymptotic SOPs of SC and EGC are rewritten as

$$P_{out_SC} = \frac{M! \bar{\gamma}_E^M}{\bar{\gamma}_B^M \det(\mathbf{U})} \sum_{k=0}^M \frac{1}{\left(1 + \sum_{k=1}^M \frac{\eta_m^2}{1 - \eta_m^2}\right)^k} \frac{1}{(M-k)!} \left(\frac{2^{R_s} - 1}{\bar{\gamma}_E}\right)^{M-k} 2^{R_s k} + o\left(\frac{1}{\bar{\gamma}_B^M}\right) \quad (39)$$

and

$$P_{out_EGC} = \frac{M! (2M)^M \bar{\gamma}_E^M}{(2M)! \bar{\gamma}_B^M \det(\mathbf{U})} \sum_{k=0}^M \frac{2^{R_s k}}{(M-k)! \left(1 + \sum_{k=1}^M \frac{\eta_m^2}{1 - \eta_m^2}\right)^k} \left(\frac{2^{R_s} - 1}{\bar{\gamma}_E}\right)^{M-k} + o\left(\frac{1}{\bar{\gamma}_B^M}\right). \quad (40)$$

It can be observed that (38), (39), and (40) are respectively the lower SOP bounds for MRC, SC and EGC, when the main and eavesdropper channels are correlated. Moreover, these equations coincide with (17), (26) and (28) with $\lambda_e^2 = 1$. Also, the upper SOP bounds correspond to the case of $\lambda_e^2 = 0$, and they have been obtained in (29), (30), and (31).

IV. SOP OF TAS WITH THE MULTI-ANTENNA EAVESDROPPER

Multiple antennas technique can be applied at both the base station and the terminals at the legitimate receiver and the eavesdropper. It is therefore necessary to investigate the SOP of a MIMO system. In addition, considering that the multi-antenna eavesdropper tries to overhear the legitimate information as much as possible, we only consider the case when MRC is deployed at the eavesdropper. Moreover, due to constraints on cost and complexity, a single RF chain is equipped at the transmitter. Only one transmit antenna is selected to forward the information. It is worth mentioning that the TAS technique has been approved by IEEE 802.16 for WiMAX and LTE-Advanced [33] since it can achieve full diversity at low cost and low implementation complexity in Rayleigh fading channels [34]. Hence, under both cases of with or without eavesdropper's CSI, the asymptotic SOP expressions of TAS/MRC, TAS/SC, and TAS/EGC are derived over correlated Rayleigh fading channels in the following. We comment that while the SOP for TAS with diversity receptions was studied for correlated legitimate channels and

correlated eavesdropper channels [11], the effects of correlations between the multi-branch main channels and the multi-branch eavesdropper channels have not been investigated.

A. Without Eavesdropper's CSI

When the eavesdropper's CSI is unavailable to the transmitter, the transmit antenna having the maximum SNR at the legitimate receiver is selected, and it can be expressed as [35]

$$n^* = \arg \max_{1 \leq n \leq N_t} \gamma_{s_n, B} \quad (41)$$

where $\gamma_{s_n, B}$ is determined by the specific combining scheme deployed at the legitimate receiver. When MRC, SC, and EGC are applied, $\gamma_{s_n, B}$ is respectively denoted by $\gamma_{s_n, B}^{MRC}$, $\gamma_{s_n, B}^{SC}$ and $\gamma_{s_n, B}^{EGC}$.

1) *MRC at the Legitimate Receiver:* Note when the eavesdropper's channel is independent of the main channels, the selected antenna n^* is a random antenna for eavesdropper E . But when the eavesdropper's channel is correlated with the main channels, the SNR at the eavesdropper $\gamma_{s_{n^*}, E}^{MRC}$ is correlated with the SNR at the legitimate receiver $\gamma_{s_{n^*}, B}^{MRC}$. Then conditioned on $x_0^2 + y_0^2 = t$, the SNR at the eavesdropper, $\gamma_{s_{n^*}, E}^{MRC}$, has a noncentral chi-square distribution $\chi_{2N_E} \left(\sqrt{N_E \bar{\gamma}_E \lambda_e^2 t}, \frac{\bar{\gamma}_E (1 - \lambda_e^2)}{2} \right)$, and the conditional PDF of $\gamma_{s_{n^*}, E}^{MRC}$ is given by

$$f_{\gamma_{s_{n^*}, E}^{MRC} | T} (y | t) = \frac{\exp \left(-\frac{y + N_E \bar{\gamma}_E \lambda_e^2 t}{\bar{\gamma}_E (1 - \lambda_e^2)} \right)}{\bar{\gamma}_E (1 - \lambda_e^2)} \left(\frac{y}{N_E \bar{\gamma}_E \lambda_e^2 t} \right)^{\frac{N_E - 1}{2}} I_{N_E - 1} \left(2 \sqrt{\frac{N_E \lambda_e^2 t y}{\bar{\gamma}_E (1 - \lambda_e^2)^2}} \right). \quad (42)$$

The conditional PDF of $\gamma_{s_{n^*}, B}^{MRC}$ has been derived in (69). Then with the help of (42) and (69), the joint PDF of $\gamma_{s_{n^*}, B}^{MRC}$ and $\gamma_{s_{n^*}, E}^{MRC}$ is given in the following lemma.

Lemma 1: The joint PDF of $\gamma_{s_{n^*}, B}^{MRC}$ and $\gamma_{s_{n^*}, E}^{MRC}$ can be obtained as

$$f_{\gamma_{s_{n^*}, B}^{MRC}, \gamma_{s_{n^*}, E}^{MRC}} (x, y) = \left(\frac{1}{\Gamma(M+1) \det(\mathbf{U})} \right)^{N_t - 1} \frac{N_t \prod_{m=1}^M \frac{1}{1 - \eta_m^2} \left(\frac{1}{1 - \lambda_e^2} \right)^{N_E}}{\Gamma(M) \bar{\gamma}_B^{MN_t} \bar{\gamma}_E^{N_E} \Gamma(N_E) \alpha} x^{MN_t - 1} \\ \times y^{N_E - 1} \exp \left(-\frac{y}{\bar{\gamma}_E (1 - \lambda_e^2)} \right) {}_1F_1 \left(1; N_E; \frac{N_E \lambda_e^2 y}{\alpha \bar{\gamma}_E (1 - \lambda_e^2)^2} \right) + o \left(\frac{x^{MN_t - 1}}{\bar{\gamma}_B^{MN_t}} \right). \quad (43)$$

Proof: The derivation is presented in Appendix C. According to (10) and (43), the asymptotic SOP of TAS/MRC is calculated as

$$P_{out_MRC}^{TAS} (R_s) = \Pr \left(\frac{\gamma_{s_{n^*}, B}^{MRC} + 1}{\gamma_{s_{n^*}, E}^{MRC} + 1} \leq 2^{R_s} \right) = \int_0^\infty \int_0^{2^{R_s} (y+1) - 1} f_{\gamma_{s_{n^*}, B}^{MRC}, \gamma_{s_{n^*}, E}^{MRC}} (x, y) dx dy \\ = \frac{1}{\prod_{m=1}^M (1 - \eta_m^2) \det(\mathbf{U})^{N_t - 1} \Gamma^{N_t} (M+1) \Gamma(N_E) \alpha \bar{\gamma}_B^{MN_t}} \sum_{\omega=0}^{MN_t} \binom{MN_t}{\omega} (2^{R_s} - 1)^{MN_t - \omega} \\ \times \Gamma(N_E + \omega) \left(2^{R_s} \bar{\gamma}_E (1 - \lambda_e^2) \right)^\omega {}_2F_1 \left(1, N_E + \omega; N_E; \frac{N_E \lambda_e^2}{\alpha (1 - \lambda_e^2)} \right) + o \left(\frac{1}{\bar{\gamma}_B^{MN_t}} \right). \quad (44)$$

As $\eta_m = 0$, $\lambda_e = 0$, $\det(\mathbf{U}) = 1$, and all channels are independent, eq. (44) is reduced to [35, eq. (27)] over Rayleigh fading. This demonstrates the generality for our result. As $\bar{\gamma}_E \gg 1$, the asymptotic SOP of TAS/MRC is rewritten as

$$P_{out_MRC}^{TAS}(R_s) = \frac{\Gamma(MN_t + N_E) (\bar{\gamma}_E 2^{R_s} (1 - \lambda_e^2))^{MN_t}}{\prod_{m=1}^M (1 - \eta_m^2) (\det(\mathbf{U}))^{N_t-1} \Gamma^{N_t}(M+1) \Gamma(N_E) \alpha \bar{\gamma}_B^{MN_t}} \times {}_2F_1\left(1, MN_t + N_E; N_E; \frac{N_E \lambda_e^2}{\alpha (1 - \lambda_e^2)}\right) + o\left(\frac{1}{\bar{\gamma}_B^{MN_t}}\right). \quad (45)$$

Specially, as $N_E = 1$, no combining schemes are deployed at the eavesdropper,

${}_1F_1\left(1; N_E; \frac{N_E \lambda_e^2 y}{\alpha \bar{\gamma}_E (1 - \lambda_e^2)^2}\right) = \exp\left(\frac{N_E \lambda_e^2 y}{\alpha \bar{\gamma}_E (1 - \lambda_e^2)^2}\right)$. The asymptotic SOP of TAS with single antenna eavesdropper is given by

$$P_{out_MRC}^{TAS}(R_s) = \frac{\Gamma(MN_t + 1) (\bar{\gamma}_E 2^{R_s} (1 - \lambda_e^2))^{MN_t}}{\Gamma^{N_t}(M+1) \det^{N_t}(\mathbf{U}) \bar{\gamma}_B^{MN_t}} \left(\frac{\sum_{m=1}^M \frac{\eta_m^2}{1 - \eta_m^2} + \frac{\lambda_e^2}{1 - \lambda_e^2}}{\sum_{m=1}^M \frac{\eta_m^2}{1 - \eta_m^2} + 1} \right)^{MN_t} + o\left(\frac{1}{\bar{\gamma}_B^{MN_t}}\right). \quad (46)$$

According to (45) and (46), the impact of the eavesdropper antenna number N_E on SOP is

$$\frac{P_{out_MRC}^{TAS}(R_s)}{P_{out_MRC}^{TAS}(R_s)_{N_E=1}} = \frac{\Gamma(MN_t + N_E) \left(\sum_{m=1}^M \frac{\eta_m^2}{1 - \eta_m^2} + 1 \right)^{MN_t+1}}{\Gamma(N_E) \left(\sum_{m=1}^M \frac{\eta_m^2}{1 - \eta_m^2} + \frac{\lambda_e^2}{1 - \lambda_e^2} \right)^{MN_t}} {}_2F_1\left(1, MN_t + N_E; N_E; \frac{N_E \lambda_e^2}{\alpha (1 - \lambda_e^2)}\right). \quad (47)$$

It can be easily found that the secrecy array gain decreases with an increase of N_E . In addition, since the impact of correlation coefficient on SOP has been analyzed and has the similar result as single-antenna eavesdropper, we do not repeat the analysis.

2) *SC at the Legitimate Receiver*: When SC is applied at the legitimate receiver, we can use the same method as described in Appendix C to obtain the joint PDF of $\gamma_{s_n^*, B}^{SC}$ and $\gamma_{s_n^*, E}^{MRC}$. The approximate SOP of TAS/SC is given by

$$P_{out_SC}^{TAS}(R_s) = \frac{1}{\prod_{m=1}^M (1 - \eta_m^2) \det(\mathbf{U})^{N_t-1} \Gamma(N_E) \alpha \bar{\gamma}_B^{MN_t}} \sum_{\omega=0}^{MN_t} \binom{MN_t}{\omega} (2^{R_s} - 1)^{MN_t - \omega} \times \Gamma(N_E + \omega) (2^{R_s} \bar{\gamma}_E (1 - \lambda_e^2))^\omega {}_2F_1\left(1, N_E + \omega; N_E; \frac{N_E \lambda_e^2}{\alpha (1 - \lambda_e^2)}\right) + o\left(\frac{1}{\bar{\gamma}_B^{MN_t}}\right). \quad (48)$$

As $\eta_m = 0$ and $\lambda_e = 0$, eq. (48) is reduced to [35, eq. (33)] over Rayleigh fading. This demonstrates the generality for our result.

3) *EGC at the Legitimate Receiver*: When EGC is applied at the legitimate receiver, we can also use the same method as described in Appendix C to obtain the joint PDF of $\gamma_{s_n^*,B}^{EGC}$ and $\gamma_{s_n^*,E}$. The approximate SOP of TAS/EGC is given by

$$\begin{aligned}
P_{out_EGC}^{TAS}(R_s) &= \frac{(2M)^{MN_t}}{\Gamma^{N_t}(2M+1) \prod_{m=1}^M (1-\eta_m^2) \det^{N_t-1}(\mathbf{U}) \Gamma(N_E) \alpha \bar{\gamma}_B^{MN_t}} \\
&\times \sum_{\omega=0}^{MN_t} \binom{MN_t}{\omega} \Gamma(N_E + \omega) (2^{R_s} - 1)^{MN_t - \omega} \left(2^{R_s} \bar{\gamma}_E (1 - \lambda_e^2)\right)^\omega \\
&\times {}_2F_1\left(1, N_E + \omega; N_E; \frac{N_E \lambda_e^2}{\alpha(1 - \lambda_e^2)}\right) + o\left(\frac{1}{\bar{\gamma}_B^{MN_t}}\right). \tag{49}
\end{aligned}$$

Remark 4: From (44), (48), and (49), the diversity order for three combining schemes is $N_t M$. Moreover, $P_{out_MRC}^{TAS}(R_s) > P_{out_EGC}^{TAS}(R_s) > P_{out_SC}^{TAS}(R_s)$. Also $P_{out_MRC}^{TAS}(R_s) / P_{out_EGC}^{TAS}(R_s) = \frac{(\Gamma(2M+1))^{N_t}}{(2M)^{MN_t} \Gamma^{N_t}(M+1)}$ and $P_{out_MRC}^{TAS}(R_s) / P_{out_SC}^{TAS}(R_s) = \frac{1}{\Gamma^{N_t}(M+1)}$. The gap for different combining schemes does not depend on the eavesdropper's antenna number N_E . Especially, as $N_t = 1$ and $N_E = 1$, eqs. (44), (48), and (49) are simplified to (17), (26), and (28). As $\lambda_e = 1$, eqs. (44), (48), and (49) are simplified to (38), (39), and (40).

B. With Eavesdropper's CSI

When the eavesdropper's CSI is available to the transmitter, the transmit antenna having the largest secrecy capacity is selected, and it can be expressed as [36], [37]

$$n^* = \arg \max_{1 \leq n \leq N_t} \log_2 \left(\frac{1 + \gamma_{s_n,B}}{1 + \gamma_{s_n,E}} \right). \tag{50}$$

Though secrecy outage may be avoided when the eavesdropper's CSI is available and the transmitter can adaptively adjust the transmission parameter such as transmission rate, such implementation can significantly increase the system complexity. Therefore, the transmitter may still adopt the constant rate transmission scheme, and secrecy outage can still occur.

1) *MRC at the Legitimate Receiver*: Since the antenna is selected according to the secrecy capacity, and the SNRs at the legitimate receiver from different antenna are independent, the asymptotic SOP of TAS/MRC is given by

$$P_{out_MRC}^{TAS'}(R_s) = \prod_{n=1}^{N_t} \Pr(C_{s_n} \leq R_s) \tag{51}$$

where $\Pr(C_{s_n} \leq R_s)$ denotes the SOP of random TAS, and it can be calculated as

$$\begin{aligned} \Pr(C_{s_n} \leq R_s) &= \int_0^\infty dy \int_0^{2^{R_s}(y+1)-1} f_{\gamma_{s_n,B}, \gamma_{s_n,E}}(x, y) dx \\ &= \frac{1}{\prod_{m=1}^M (1 - \eta_m^2) \Gamma(M+1) \Gamma(N_E) \bar{\gamma}_B^M \alpha} \sum_{\omega=0}^M \binom{M}{\omega} (2^{R_s} - 1)^{M-\omega} \\ &\quad \times \Gamma(N_E + \omega) (\bar{\gamma}_E 2^{R_s} (1 - \lambda_e^2))^\omega {}_2F_1\left(1, N_E + \omega; N_E; \frac{N_E \lambda_e^2}{\alpha(1 - \lambda_e^2)}\right) + o(\bar{\gamma}_B^{-M}). \end{aligned} \quad (52)$$

Substituting (52) into (53), the asymptotic SOP of TAS/MRC with eavesdropper's CSI is

$$\begin{aligned} P_{out_MRC}^{TAS'}(R_s) &= \frac{1}{\left(\prod_{m=1}^M (1 - \eta_m^2)\right)^{N_t} \Gamma^{N_t}(M+1) \Gamma^{N_t}(N_E) \bar{\gamma}_B^{MN_t} \alpha^{N_t}} \\ &\quad \times \left(\sum_{\omega=0}^M \binom{M}{\omega} (2^{R_s} - 1)^{M-\omega} \Gamma(N_E + \omega) (\bar{\gamma}_E 2^{R_s} (1 - \lambda_e^2))^\omega\right. \\ &\quad \left. \times {}_2F_1\left(1, N_E + \omega; N_E; \frac{N_E \lambda_e^2}{\alpha(1 - \lambda_e^2)}\right)\right)^{N_t} + o(\bar{\gamma}_B^{-MN_t}). \end{aligned} \quad (53)$$

As $N_E = 1$, eq. (53) can be simplified as

$$\begin{aligned} P_{out_MRC}^{TAS'}(R_s) &= \frac{1}{(\det(\mathbf{U}))^{N_t}} \left(\frac{\bar{\gamma}_E}{\bar{\gamma}_B}\right)^{MN_t} \\ &\quad \times \left[\sum_{k=0}^M \frac{1}{(M-k)!} \left(\frac{2^{R_s} \left(\sum_{m=1}^M \frac{\eta_m^2 (1 - \lambda_e^2)}{1 - \eta_m^2} + 1\right)}{\left(\sum_{m=1}^M \frac{\eta_m^2}{1 - \eta_m^2} + 1\right)}\right)^k \left(\frac{2^{R_s} - 1}{\bar{\gamma}_E}\right)^{M-k} \right]^{N_t} + o(\bar{\gamma}_B^{-MN_t}). \end{aligned} \quad (54)$$

From (53) and (54), we can easily find the secrecy diversity order is MN_t , which does not depend on the eavesdropper antenna number N_E . To further investigate the impact of N_E on the SOP, with $\bar{\gamma}_E \gg 1$, eq. (53) can be rewritten as

$$\begin{aligned} P_{out_MRC}^{TAS'}(R_s) &= \frac{\Gamma^{N_t}(N_E + M) 2^{R_s MN_t} (\bar{\gamma}_E (1 - \lambda_e^2))^{MN_t}}{\left(\prod_{m=1}^M (1 - \eta_m^2)\right)^{N_t} \Gamma^{N_t}(M+1) \Gamma^{N_t}(N_E) \bar{\gamma}_B^{MN_t} \alpha^{N_t}} \\ &\quad \times \left({}_2F_1\left(1, N_E + M; N_E; \frac{N_E \lambda_e^2}{\alpha(1 - \lambda_e^2)}\right)\right)^{N_t} + o(\bar{\gamma}_B^{-MN_t}) \end{aligned} \quad (55)$$

which will be used to discuss the gap of different TAS schemes.

2) *SC at the Legitimate Receiver*: Similar to MRC, according to (26), the asymptotic SOP of TAS/SC is given by

$$P_{out_SC}^{TAS'}(R_s) = \left(\frac{1}{\left(\prod_{m=1}^M (1 - \eta_m^2) \right) \Gamma(N_E) \bar{\gamma}_B^M \alpha} \right)^{N_t} \left(\sum_{\omega=0}^M \binom{M}{\omega} (2^{R_s} - 1)^{M-\omega} \Gamma(N_E + \omega) \right. \\ \left. \times \left(\bar{\gamma}_E 2^{R_s} (1 - \lambda_e^2) \right)^\omega {}_2F_1 \left(1, N_E + \omega; N_E; \frac{N_E \lambda_e^2}{\alpha (1 - \lambda_e^2)} \right) \right)^{N_t} + o(\bar{\gamma}_B^{-MN_t}). \quad (56)$$

3) *EGC at the Legitimate Receiver*: Similar to MRC, according to (28), the asymptotic SOP of TAS/EGC is given by

$$P_{out_EGC}^{TAS'}(R_s) = \left(\frac{(2M)^M}{\left(\prod_{m=1}^M (1 - \eta_m^2) \right) \Gamma(2M + 1) \Gamma(N_E) \bar{\gamma}_B^M \alpha} \right)^{N_t} \\ \times \left(\sum_{\omega=0}^M \binom{M}{\omega} (2^{R_s} - 1)^{M-\omega} \Gamma(N_E + \omega) \left(\bar{\gamma}_E 2^{R_s} (1 - \lambda_e^2) \right)^\omega \right. \\ \left. \times {}_2F_1 \left(1, N_E + \omega; N_E; \frac{N_E \lambda_e^2}{\alpha (1 - \lambda_e^2)} \right) \right)^{N_t} + o(\bar{\gamma}_B^{-MN_t}). \quad (57)$$

As $N_t = 1$, eqs. (53), (56), and (58) specialize to (45), (48), and (49), respectively. Note that when $\eta_m = 1$, and $\lambda_e = 1$, all the channels are fully correlated. In this case, the SOP of TAS/MRC is given by

$$P_{out}^{TAS'} = \left(1 - \exp \left(-\frac{2^{R_s} - 1}{\varepsilon \bar{\gamma}_B - 2^{R_s} N_E \bar{\gamma}_E} \right) \right)^{N_t} \quad (58)$$

where ε is equal to M for EGC and MRC, and equal to 1 for SC. The inequality $\varepsilon \bar{\gamma}_B > 2^{R_s} N_E \bar{\gamma}_E$ is required for (58); otherwise, secrecy can not be guaranteed.

C. Discussion

TAS with eavesdropper's CSI requires the transmitter to obtain instantaneous CSI for all channels, but TAS without eavesdropper's CSI only requires the main channels instantaneous CSI. In addition, it can be seen from (44)-(58) that with or without eavesdropper's CSI, regardless

which combining scheme is deployed, the secrecy diversity order is MN_t . The difference lies in the secrecy array gain. As $\bar{\gamma}_E \gg 1$, the ratio of (45) and (55) can be written as

$$\begin{aligned} \frac{P_{out_MRC}^{TAS}(R_s)}{P_{out_MRC}^{TAS'}(R_s)} &= \frac{\Gamma(MN_t + N_E) \Gamma^{N_t-1}(N_E)}{\Gamma^{N_t}(M + N_E)} \left(\frac{\left(1 + \sum_{m=1}^M \frac{\eta_m^2}{1-\eta_m^2} + \frac{N_E \lambda_e^2}{1-\lambda_e^2}\right)}{\left(1 + \sum_{m=1}^M \frac{\eta_m^2}{1-\eta_m^2}\right)} \right)^{N_t-1} \\ &\times \frac{{}_2F_1\left(1, MN_t + N_E; N_E; \frac{N_E \lambda_e^2}{\alpha(1-\lambda_e^2)}\right)}{\left({}_2F_1\left(1, M + N_E; N_E; \frac{N_E \lambda_e^2}{\alpha(1-\lambda_e^2)}\right)\right)^{N_t}}. \end{aligned} \quad (59)$$

In (59), the first part can be expressed as

$$\frac{\Gamma(MN_t + N_E) \Gamma^{N_t-1}(N_E)}{\Gamma^{N_t}(M + N_E)} = \frac{\underbrace{(MN_t + N_E - 1) \cdots (N_E + 1) N_E}_{MN_t} \times \Gamma^{N_t}(N_E)}{\left(\underbrace{(M + N_E - 1) \cdots (N_E + 1) N_E}_M\right)^{N_t} \times \Gamma^{N_t}(N_E)} \geq 1. \quad (60)$$

Note in (60) as $N_t = 1$, the equality is satisfied. Moreover, the second part of (59),

$$\left(\frac{1 + \sum_{m=1}^M \frac{\eta_m^2}{1-\eta_m^2} + \frac{N_E \lambda_e^2}{1-\lambda_e^2}}{1 + \sum_{m=1}^M \frac{\eta_m^2}{1-\eta_m^2}} \right)^{N_t-1}, \text{ is also larger than 1, and the third part } \frac{{}_2F_1\left(1, MN_t + N_E; N_E; \frac{N_E \lambda_e^2}{\alpha(1-\lambda_e^2)}\right)}{\left({}_2F_1\left(1, M + N_E; N_E; \frac{N_E \lambda_e^2}{\alpha(1-\lambda_e^2)}\right)\right)^{N_t}} \simeq 1.$$

Obviously, the gap is increased with N_t . For the special case of $N_E = 1$, eq. (59) is simplified to

$$\frac{P_{out_MRC}^{TAS}(R_s)}{P_{out_MRC}^{TAS'}(R_s)} = \frac{(MN_t)!}{(M!)^{N_t}} \quad (61)$$

where the identity ${}_2F_1(-n, 1; 1; -z) = (1+z)^n$ is used [28, eq. (9.121.1)] to obtain (61). Similar to (60), we have $(MN_t)! \geq (M!)^{N_t}$. Then $P_{out_MRC}^{TAS}(R_s) \geq P_{out_MRC}^{TAS'}(R_s)$. In addition, with SC and EGC at the legitimate receiver, using (48), (49), (56), and (58), similar analytical results can be obtained. Due to space limitation, we omit the analyse here.

Remark 5: The SOP of TAS with eavesdropper's CSI outperforms the case without eavesdropper's CSI, regardless which combining scheme is deployed at the legitimate receiver. As $\bar{\gamma}_B \rightarrow \infty$, the SOP gap with eavesdropper CSI and without eavesdropper CSI is increased with N_t , and it has no relationship with N_E .

V. SIMULATION RESULTS

In this section, we present numerical and simulation results to verify our analysis. All the links are assumed to experience Rayleigh flat fading. Without loss of generality, we set $R_s = 1$ bit/sec/Hz.

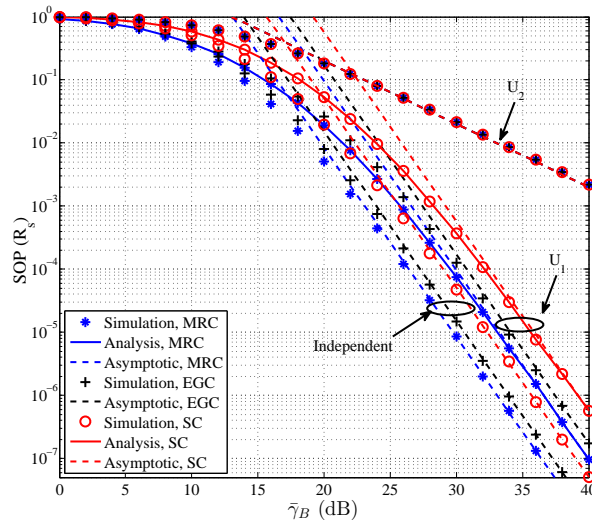


Fig. 2. The SOP versus $\bar{\gamma}_B$ under the case of CMC. $M = 3$, $N_t = 1$, $N_E = 1$, $\lambda_e = 0$, and $\bar{\gamma}_E = 10$ dB.

When the multi-antenna main channels are correlated and independent of the eavesdropper channel, the SOPs of MRC, SC, and EGC are plotted in Fig. 2, where \mathbf{U}_1 denotes the correlation matrix at the multi-antenna legitimate receiver, and it is given by

$$\mathbf{U}_1 = \begin{pmatrix} 1 & 0.765 & -0.8075 \\ 0.765 & 1 & -0.8550 \\ -0.8075 & -0.8550 & 1 \end{pmatrix} \quad (62)$$

where $\det(\mathbf{U}_1) = 0.088$. In \mathbf{U}_1 , the coefficients $\eta_1 = 0.8$, $\eta_2 = 0.85$, $\eta_3 = -0.95$. \mathbf{U}_2 denotes the case that the main channels are completely correlated, namely $\eta_m = 1$. The curves named independent in Fig. 2 represent the case when all the channels are independent. We can find that compared to the case where main channels are independent, CMC degrades the SOP. This is because when the main channels are independent, i.e. $\eta_m = 0$, the determinant of correlation matrix is 1, and is greater than $\det(\mathbf{U}_1)$. Namely, antenna correlation at the legitimate receiver has a negative effect on SOP, as shown in Remark 1. In addition, we can observe that MRC is better than EGC and SC except for the completely correlated case. It is because when the main channels are completely correlated, only one effective channel plays a role for diversity reception. Thus, for the completely correlated case, SC, EGC and MRC have the same SOP performance. Also, it can be seen that simulation results coincide with the analytical results. When $\bar{\gamma}_B$ is increased, the asymptotic results converge to the simulation and analytical results, which verifies our analysis.

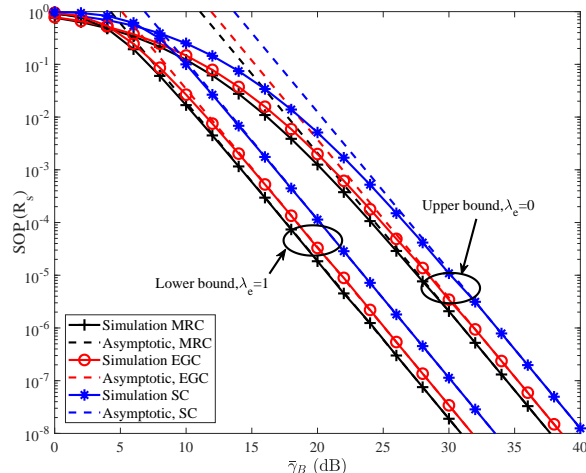


Fig. 3. The lower and upper bounds of SOP versus $\bar{\gamma}_B$. $M = 3$, $N_t = 1$, $N_E = 1$, and $\bar{\gamma}_E = 5$ dB.

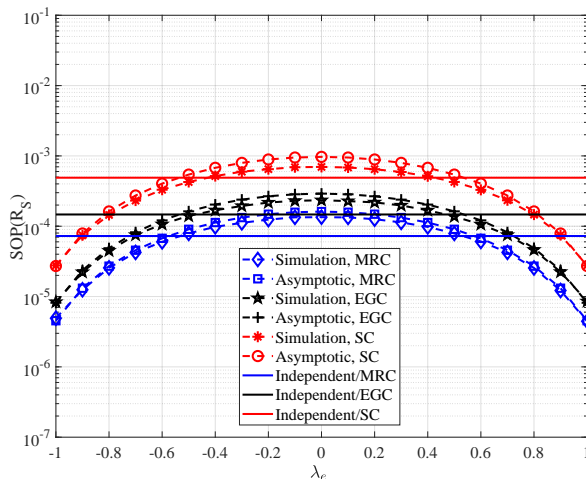


Fig. 4. The impact of λ_e on SOP. $M = 3$, $N_t = 1$, $\bar{\gamma}_B = 20$ dB, and $\bar{\gamma}_E = 3$ dB.

The lower and upper bounds of SOP for MRC, SC, and EGC are illustrated in Fig. 3. The main channel correlation matrix is U_1 . We can observe that the SOP with $\lambda_e = 1$ is clearly better than that with $\lambda_e = 0$, which verifies our prediction that the correlation between the main channels and eavesdropper channels has a positive impact on SOP when the average SNR at the legitimate receiver is larger than that at the eavesdropper. When $\bar{\gamma}_B$ is increased, the simulation results converge to the asymptotic results. In addition, it can be found that all the asymptotic curves have the same slope. This is because all the combining schemes have the same secrecy diversity order M , as predicted by our analysis.

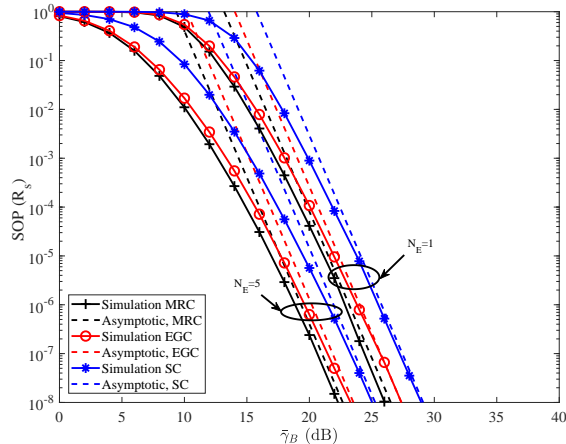


Fig. 5. The SOP of TAS without the eavesdropper's CSI. $\lambda_e = 0.8$, $N_t = 2$, and $\bar{\gamma}_E = 5$ dB.

The impact of λ_e on SOP is examined in Fig. 4, where the dashed line denotes the scenario when all the channels are correlated and the main channels correlation matrix is \mathbf{U}_3 ; the solid line denotes the scenario all channels are independent. \mathbf{U}_3 is given by

$$\mathbf{U}_3 = \begin{pmatrix} 1 & -0.42 & 0.48 \\ -0.42 & 1 & -0.56 \\ 0.48 & -0.56 & 1 \end{pmatrix}. \quad (63)$$

In \mathbf{U}_3 , the correlation coefficients are $\eta_1 = 0.6$, $\eta_2 = -0.7$, $\eta_3 = 0.8$, and $\det(\mathbf{U}_3) = 0.5054$. It can be seen that as λ_e is small, the SOP performance of the scenario when all the channels are independent is better than the scenario when all the channels are correlated. But as λ_e is increased, the contrary result is obtained. In other words, the SOP when all the channels are correlated can be lower than that when all the channels are independent, which agree with the discussion in Remark 3.

For different number of antennas at the eavesdropper, with or without the eavesdropper's CSI, the SOPs of TAS with MRC, SC, and EGC are illustrated in Fig. 5, where the main channel correlation matrix is \mathbf{U}_1 . The SOP is increased when the number of antennas at the eavesdropper is increased, which verifies our secrecy analysis in Section IV. Also, we can observe all the curves have the same slope. It is because no matter with or without eavesdropper's CSI, the secrecy diversity order is $N_t M$ and has no relationship with N_E .

When multiple antennas are deployed at the transmitter and the eavesdropper, the SOPs of TAS/MRC with or without eavesdropper's CSI are plotted in Fig. 6, where the main channels have

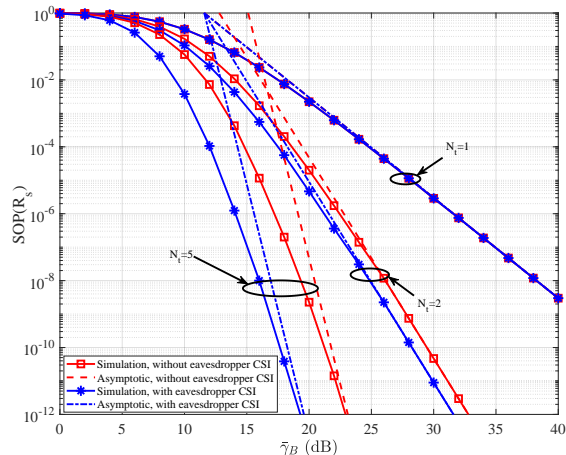


Fig. 6. The SOP of TAS/MRC with or without the eavesdropper's CSI. $M = 3$, $N_E = 3$, $\lambda_e = 0.5$, and $\bar{\gamma}_E = 5$ dB.

correlation matrix U_3 . It can be seen that the SOP of TAS with eavesdropper's CSI outperforms that without eavesdropper's CSI. This is because TAS with eavesdropper selects the antenna according to the maximum secrecy capacity. Also, we can find that as $N_t = 1$, TAS with eavesdropper's CSI has the same SOP as TAS without eavesdropper's CSI as expected. The gap of SOP for the two TAS cases is increased with N_t , which verifies our analysis in Remark 5.

VI. CONCLUSION

We considered a comprehensive secure communication system model with generalized correlation structure. The impacts of both antenna correlation and channel correlation between the legitimate receiver and eavesdropper on the SOP were investigated and quantified in detail. The findings suggest that the antenna correlation at the legitimate receiver alone is detrimental to the SOP. However, when the average SNR at the legitimate is greater than that at the eavesdropper, the correlation between the main and eavesdropper's channels can enhance the SOP. Finally, for an eavesdropper with multiple antennas, the gaps of SOP for TAS with and without eavesdropper's CSI increase with the number of transmitter antennas.

APPENDIX A

APPROXIMATE CONDITIONAL PDF OF $\gamma_{s_n, B}^{MRC}$

Assuming $T = X_{n,0}^2 + Y_{n,0}^2$, $X_{n,0} = x_0$, and $Y_{n,0} = y_0$. Conditioned on $x_0^2 + y_0^2 = t$, the MGF of $\gamma_{s_n, B}^{MRC}$ can be expressed as [38]

$$\begin{aligned}\phi_{\gamma_{s_n, B}^{MRC}|T}(s|t) &= E\left(\exp\left(-s\sum_{m=1}^M\gamma_{s_n, b_m}\right)\middle|t\right) = \prod_{m=1}^M E(\exp(-s\gamma_{s_n, b_m})|t) \\ &= \prod_{m=1}^M \phi_{\gamma_{s_n, b_m}|T}(s|t)\end{aligned}\quad (64)$$

where $\phi_{\gamma_{s_n, b_m}|T}(s|t)$ denotes MGF of γ_{s_n, b_m} conditioned on T . Note that the conditional PDF of γ_{s_n, b_m} can be obtained by differentiating (22) with respect to y , and it is given by

$$f_{\gamma_{s_n, b_m}|T}(y|t) = \frac{\exp\left(-\frac{\eta_m^2 t}{1-\eta_m^2}\right)}{\bar{\gamma}_B(1-\eta_m^2)} \exp\left(-\frac{y}{\bar{\gamma}_B(1-\eta_m^2)}\right) I_0\left(2\sqrt{\frac{\eta_m^2 ty}{\bar{\gamma}_B(1-\eta_m^2)^2}}\right). \quad (65)$$

According to (65), the MGF of γ_{s_n, b_m} conditioned on T can be calculated as

$$\begin{aligned}\phi_{\gamma_{s_n, b_m}|T}(s|t) &= \int_0^\infty e^{-sy} f_{\gamma_{s_n, b_m}|T}(y|t) dy \\ &= \frac{\exp\left(-\frac{\eta_m^2 t}{1-\eta_m^2}\right)}{\bar{\gamma}_B(1-\eta_m^2)} \int_0^\infty \exp\left(-\left(s + \frac{1}{\bar{\gamma}_B(1-\eta_m^2)}\right)y\right) I_0\left(2\sqrt{\frac{\eta_m^2 ty}{\bar{\gamma}_B(1-\eta_m^2)^2}}\right) dy \\ &= \frac{\exp\left(-\left(\frac{\eta_m^2 \bar{\gamma}_B t s}{(1+s\bar{\gamma}_B(1-\eta_m^2))}\right)\right)}{\bar{\gamma}_B(1-\eta_m^2)s+1}.\end{aligned}\quad (66)$$

As $\bar{\gamma}_B \rightarrow \infty$, $s\bar{\gamma}_B(1-\eta_m^2) \gg 1$. Thus the asymptotic conditional MGF of γ_{s_n, b_m} is

$$\phi_{\gamma_{s_n, b_m}|T}(s|t) \simeq \frac{\exp\left(-\left(\frac{\eta_m^2 t}{(1-\eta_m^2)}\right)\right)}{\bar{\gamma}_B(1-\eta_m^2)s}.\quad (67)$$

Then, the asymptotic conditional MGF $\gamma_{s_n, B}^{MRC}$ can be obtained as

$$\phi_{\gamma_{s_n, B}^{MRC}|T}(s|t) = \frac{\exp\left(-\sum_{m=1}^M \frac{\eta_m^2 t}{(1-\eta_m^2)}\right)}{\bar{\gamma}_B^M} \prod_{m=1}^M \frac{1}{(1-\eta_m^2)s^M}.\quad (68)$$

Performing the inverse Laplace transform for (68), we obtain the conditional PDF of $\gamma_{s_n, B}^{MRC}$ as

$$f_{\gamma_{s_n, B}^{MRC}|T}(x|t) = \mathcal{L}^{-1}\left(\phi_{\gamma_{s_n, B}^{MRC}|T}(s|t)\right) = \frac{\exp\left(-\sum_{m=1}^M \frac{\eta_m^2 t}{(1-\eta_m^2)}\right) \prod_{m=1}^M \frac{1}{(1-\eta_m^2)} x^{M-1}}{\Gamma(M) \bar{\gamma}_B^M}.\quad (69)$$

APPENDIX B

APPROXIMATE CONDITIONAL PDF OF $\gamma_{s_n, B}^{EGC}$

According to (27), to derive the PDF of $\gamma_{s_n, B}^{EGC}$, we are required to derive the PDF of $\sqrt{\gamma_{s_n, B}^{EGC}}$. Let $Z = \sqrt{\gamma_{s_n, B}^{EGC}} = \sum_{m=1}^M \sqrt{\frac{\gamma_{s_n, bm}}{M}}$, conditioned on $x_0^2 + y_0^2 = t$, the MGF of Z is given by

$$\begin{aligned} \phi_{Z|T}(s|t) &= E \left(\exp \left(-s \left(\sum_{m=1}^M \sqrt{\frac{\gamma_{s_n, bm}}{M}} \right) \right) \middle| t \right) = \prod_{m=1}^M E \left(\exp \left(-s \sqrt{\frac{\gamma_{s_n, bm}}{M}} \right) \middle| t \right) \\ &= \prod_{m=1}^M \phi_{\sqrt{\frac{\gamma_{s_n, bm}}{M}}|T}(s|t) \end{aligned} \quad (70)$$

where $\phi_{\sqrt{\frac{\gamma_{s_n, bm}}{M}}|T}(s|t)$ denotes the MGF of $\sqrt{\frac{\gamma_{s_n, bm}}{M}}$ conditioned on T . According to (65), performing a variable transformation, and the PDF of $\sqrt{\gamma_{s_n, bm}}$ conditioned on T is given by

$$f_{\sqrt{\gamma_{s_n, bm}}|T}(x|t) = \frac{2 \exp \left(-\frac{\eta_m^2 t}{1-\eta_m^2} \right)}{\bar{\gamma}_B (1-\eta_m^2)} x \exp \left(-\frac{x^2}{\bar{\gamma}_B (1-\eta_m^2)} \right) I_0 \left(2 \sqrt{\frac{\eta_m^2 t x^2}{\bar{\gamma}_B (1-\eta_m^2)^2}} \right). \quad (71)$$

Thus, $\phi_{\sqrt{\frac{\gamma_{s_n, bm}}{M}}|T}(s|t)$ can be calculated as

$$\begin{aligned} \phi_{\sqrt{\frac{\gamma_{s_n, bm}}{M}}|T}(s|t) &= \int_0^\infty \exp \left(-\frac{sx}{\sqrt{M}} \right) f_{\sqrt{\gamma_{s_n, bm}}|T}(x|t) dx \\ &= \int_0^\infty \exp \left(-\frac{sx}{\sqrt{M}} \right) \frac{2 \exp \left(-\frac{\eta_m^2 t}{1-\eta_m^2} \right)}{\bar{\gamma}_B (1-\eta_m^2)} x \exp \left(-\frac{x^2}{\bar{\gamma}_B (1-\eta_m^2)} \right) I_0 \left(\sqrt{\frac{\eta_m^2 t x^2}{\bar{\gamma}_B (1-\eta_m^2)}} \right) dx. \end{aligned} \quad (72)$$

As $\bar{\gamma}_B \rightarrow \infty$, $I_0 \left(\sqrt{\frac{\eta_m^2 t x^2}{\bar{\gamma}_B (1-\eta_m^2)}} \right) \simeq 1$, and $\exp \left(-\frac{x^2}{\bar{\gamma}_B (1-\eta_m^2)} \right) \simeq 1$. Thus, the MGF of $\sqrt{\frac{\gamma_{s_n, bm}}{M}}$ conditioned on T is approximated as

$$\phi_{\sqrt{\frac{\gamma_{s_n, bm}}{M}}|T}(s|t) \simeq \int_0^\infty x \exp \left(-\frac{sx}{\sqrt{M}} \right) \frac{2 \exp \left(-\frac{\eta_m^2 t}{1-\eta_m^2} \right)}{\bar{\gamma}_B (1-\eta_m^2)} dx = \frac{2M \exp \left(-\frac{\eta_m^2 t}{1-\eta_m^2} \right)}{\bar{\gamma}_B (1-\eta_m^2) s^2}. \quad (73)$$

Substituting (73) into (70), we obtain

$$\phi_{Z|T}(s|t) \simeq \frac{(2M)^M \exp \left(-\sum_{k=1}^M \frac{\eta_m^2 t}{1-\eta_m^2} \right)}{\bar{\gamma}_B^M \prod_{k=1}^M (1-\eta_m^2) s^{2M}}. \quad (74)$$

Performing the inverse Laplace transform of (75), we obtain the PDF of Z conditioned on T as

$$f_{Z|T}(z|t) \simeq \frac{(2M)^M \exp \left(-\sum_{k=1}^M \frac{\eta_m^2 t}{1-\eta_m^2} \right) z^{2M-1}}{\Gamma(2M) \bar{\gamma}_B^M \prod_{k=1}^M (1-\eta_m^2)}. \quad (75)$$

Since $\gamma_{s_n, B}^{EGC} = Z^2$, after a proper transformation, the PDF of $\gamma_{s_n, B}^{EGC}$ conditioned on T is

$$f_{\gamma_{s_n, B}^{EGC}|T}(x|t) \simeq \frac{(2M)^M \exp\left(-\sum_{m=1}^M \frac{\eta_m^2 t}{1-\eta_m^2}\right) x^{M-1}}{2\Gamma(2M)\bar{\gamma}_B^M \prod_{m=1}^M (1-\eta_m^2)}. \quad (76)$$

C APPROXIMATE JOINT PDF OF $\gamma_{s_n^*, B}^{MRC}$ AND $\gamma_{s_n^*, E}^{MRC}$

The PDF of $\gamma_{s_n^*, B}^{MRC}$ is given by

$$f_{\gamma_{s_n^*, B}^{MRC}}(x) = N_t \left(F_{\gamma_{s_n, B}^{MRC}}(x) \right)^{N_t-1} f_{\gamma_{s_n, B}^{MRC}}(x). \quad (77)$$

Then, the joint PDF of $\gamma_{s_n^*, B}^{MRC}$ and $\gamma_{s_n^*, E}^{MRC}$ is calculated as

$$\begin{aligned} f_{\gamma_{s_n^*, B}^{MRC}, \gamma_{s_n^*, E}^{MRC}}(x, y) &= \frac{f_{\gamma_{s_n, B}^{MRC}, \gamma_{s_n, E}^{MRC}}(x, y)}{f_{\gamma_{s_n, B}^{MRC}}(x)} N_t \left(F_{\gamma_{s_n, B}^{MRC}}(x) \right)^{N_t-1} f_{\gamma_{s_n, B}^{MRC}}(x) \\ &= N_t f_{\gamma_{s_n, B}^{MRC}, \gamma_{s_n, E}^{MRC}}(x, y) \left(F_{\gamma_{s_n, B}^{MRC}}(x) \right)^{N_t-1} \end{aligned} \quad (78)$$

where, with the help of (42), the joint PDF of $\gamma_{s_n, B}^{MRC}$ and $\gamma_{s_n, E}^{MRC}$ can be written as

$$\begin{aligned} f_{\gamma_{s_n, B}^{MRC}, \gamma_{s_n, E}^{MRC}}(x, y) &= \int_0^\infty \exp(-t) f_{\gamma_{s_n, B}^{MRC}|T}(x|t) f_{\gamma_{s_n, E}^{MRC}|T}(y|t) dt \\ &= \int_0^\infty \frac{\prod_{m=1}^M \frac{1}{1-\eta_m^2}}{\Gamma(M) \bar{\gamma}_B^M} x^{M-1} \frac{1}{\bar{\gamma}_E (1-\lambda_e^2)} \left(\frac{y}{N_E \bar{\gamma}_E \lambda_e^2 t} \right)^{\frac{N_E-1}{2}} \\ &\quad \times \exp\left(-t - \sum_{m=1}^M \frac{\eta_m^2 t}{1-\eta_m^2} - \frac{N_E \lambda_e^2 t}{(1-\lambda_e^2)}\right) I_{N_E-1} \left(2 \sqrt{\frac{N_E \lambda_e^2 t y}{\bar{\gamma}_E (1-\lambda_e^2)^2}} \right) dt \\ &= \frac{\left(\frac{1}{1-\lambda_e^2}\right)^{N_E} x^{M-1} y^{N_E-1} \exp\left(\frac{-y}{\bar{\gamma}_E (1-\lambda_e^2)}\right)}{\prod_{m=1}^M (1-\eta_m^2) \Gamma(M) \bar{\gamma}_B^M \bar{\gamma}_E^{N_E} \Gamma(N_E) \alpha} {}_1F_1 \left(1; N_E; \frac{N_E \lambda_e^2 y}{\alpha \bar{\gamma}_E (1-\lambda_e^2)^2} \right) + o\left(\frac{x^{M-1}}{\bar{\gamma}_B^M}\right) \end{aligned} \quad (79)$$

where $\alpha = 1 + \sum_{m=1}^M \frac{\eta_m^2}{1-\eta_m^2} + \frac{N_E \lambda_e^2}{(1-\lambda_e^2)}$. Both identities [28, eq. (6.643.2)] and [28, eq. (9.220.2)] are used for obtaining (79). Integrating (69) with respect to (w. r. t) t , we can obtain an approximate CDF of $\gamma_{s_n, B}^{MRC}$ as

$$F_{\gamma_{s_n, B}^{MRC}}(x) = \frac{x^M}{M! \det(\mathbf{U}) \bar{\gamma}_B^M} + o\left(\frac{x^M}{\bar{\gamma}_B^M}\right). \quad (80)$$

Substituting (80) and (79) into (78), the asymptotic joint PDF of $\gamma_{s_n^*, B}^{MRC}$ and $\gamma_{s_n^*, E}^{MRC}$ can be obtained as (43).

REFERENCES

- [1] M. Bloch, J. Barros, M. R. D. Rodrigues, and S. W. McLaughlin, "Wireless information-theoretic security," *IEEE Trans. Inf. Theory*, vol. 54, no. 6, pp. 2515–2534, June 2008.
- [2] H. Lei, C. Gao, I. S. Ansari, Y. Guo, G. Pan, and K. A. Qaraqe, "On physical-layer security over SIMO generalized- K fading channels," *IEEE Trans. Veh. Technol.*, vol. 65, no. 9, pp. 7780–7785, Sep. 2016.
- [3] X. Zhou, Z. Rezki, B. Alomair, and M. Alouini, "Achievable rates of secure transmission in Gaussian MISO channel with imperfect main channel estimation," *IEEE Trans. Commun.*, vol. 15, no. 6, pp. 4470–4485, June 2016.
- [4] F. S. Al-Qahtani, Y. Huang, S. Hessien, R. M. Radaydeh, C. Zhong, and H. M. Alnuweiri, "Secrecy analysis of MIMO wiretap channels with low-complexity receivers under imperfect channel estimation," *IEEE Trans. Inf. Forensics Security*, vol. 12, no. 2, pp. 257–270, Feb. 2017.
- [5] Y. Huang, F. S. Al-Qahtani, T. Q. Duong, and J. Wang, "Secure transmission in MIMO wiretap channels using general-order transmit antenna selection with outdated CSI," *IEEE Trans. Commun.*, vol. 63, no. 8, pp. 2959–2971, Aug. 2015.
- [6] J. Hu, Y. Cai, N. Yang, and W. Yang, "A new secure transmission scheme with outdated antenna selection," *IEEE Trans. Inf. Forensics Security*, vol. 10, no. 11, pp. 2435–2446, Nov. 2015.
- [7] V. U. Prabhu and M. R. D. Rodrigues, "On wireless channels with M -antenna eavesdroppers: Characterization of the outage probability and ϵ -outage secrecy capacity," *IEEE Trans. Inf. Forensics Security*, vol. 6, no. 3, pp. 853–860, Sep. 2011.
- [8] M. Z. I. Sarkar and T. Ratnarajah, "Enhancing security in correlated channel with maximal ratio combining diversity," *IEEE Trans. Signal Process.*, vol. 60, no. 12, pp. 6745–6751, Dec. 2012.
- [9] N. S. Ferdinand, D. B. da Costa, and M. Latva-aho, "Physical layer security in MIMO OSTBC line-of-sight wiretap channels with arbitrary transmit/receive antenna correlation," *IEEE Wireless Commun. Lett.*, vol. 2, no. 5, pp. 467–470, Oct. 2013.
- [10] K. P. Peppas, N. C. Sagias, and A. Maras, "Physical layer security for multiple-antenna systems: A unified approach," *IEEE Trans. Commun.*, vol. 64, no. 1, pp. 314–328, Jan. 2016.
- [11] N. Yang, H. A. Suraweera, I. B. Collings, and C. Yuen, "Physical layer security of TAS/MRC with antenna correlation," *IEEE Trans. Inf. Forensics Security*, vol. 8, no. 1, pp. 254–259, Jan. 2013.
- [12] H. Jeon, N. Kim, J. Choi, H. Lee, and J. Ha, "Bounds on secrecy capacity over correlated ergodic fading channels at high SNR," *IEEE Trans. Inf. Theory*, vol. 57, no. 4, pp. 1975–1983, Apr. 2011.
- [13] X. Sun, J. Wang, W. Xu, and C. Zhao, "Performance of secure communications over correlated fading channels," *IEEE Signal Process. Lett.*, vol. 19, no. 8, pp. 479–482, Aug. 2012.
- [14] G. C. Alexandropoulos and K. P. Peppas, "Secrecy outage analysis over correlated composite Nakagami- m /Gamma fading channels," *IEEE Commun. Lett.*, vol. 22, no. 1, pp. 77–80, Jan. 2018.
- [15] N. S. Ferdinand, D. B. da Costa, A. L. F. de Almeida, and M. Latva-aho, "Physical layer secrecy performance of TAS wiretap channels with correlated main and eavesdropper channels," *IEEE Wireless. Commun. Lett.*, vol. 3, no. 1, pp. 86–89, Feb. 2014.
- [16] L. Fan, X. Lei, N. Yang, T. Q. Duong, and G. K. Karagiannidis, "Secrecy cooperative networks with outdated relay selection over correlated fading channels," *IEEE Trans. Veh. Technol.*, vol. 66, no. 8, pp. 7599–7603, Aug. 2017.
- [17] L. Fan, R. Zhao, F. Gong, N. Yang, and G. K. Karagiannidis, "Secure multiple amplify-and-forward relaying over correlated fading channels," *IEEE Trans. Commun.*, vol. 65, no. 7, pp. 2811–2820, July 2017.
- [18] M. Li, H. Yin, Y. Huang, and Y. Wang, "Impact of correlated fading channels on cognitive relay networks with generalized relay selection," *IEEE Access*, vol. 6, pp. 6040–6047, Mar. 2018.

- [19] J. Zhang, B. He, T. Q. Duong, and R. Woods, "On the key generation from correlated wireless channels," *IEEE Commun. Lett.*, vol. 21, no. 4, pp. 961–964, Apr. 2017.
- [20] M.-S. Alouini, A. Abdi, and M. Kaveh, "Sum of gamma variates and performance of wireless communication systems over Nakagami-Fading channels," *IEEE Trans. Veh. Technol.*, vol. 50, no. 6, pp. 1471–1480, Nov. 2001.
- [21] A. Almradi and K. A. Hamdi, "On the outage probability of MIMO full-duplex relaying: Impact of antenna correlation and imperfect CSI," *IEEE Trans. Veh. Technol.*, vol. 66, no. 5, pp. 3957–3965, May 2017.
- [22] Y. Chen and C. Tellambura, "Distribution functions of selection combiner output in equally correlated Rayleigh, Rician, and Nakagami- m fading channels," *IEEE Trans. Commun.*, vol. 52, no. 11, pp. 1948–1956, Nov. 2004.
- [23] J. Schlenker, J. Cheng, and R. Schober, "Improving and bounding asymptotic approximations for diversity combiners in correlated generalized Rician fading," *IEEE Trans. Wireless Commun.*, vol. 13, no. 2, pp. 736–748, Feb. 2014.
- [24] X. Zhang and N. C. Beaulieu, "Performance analysis of generalized selection combining in generalized correlated Nakagami- m fading," *IEEE Trans. Commun.*, vol. 54, no. 11, pp. 2103–2112, Nov. 2006.
- [25] B. He, X. Zhou, and A. L. Swindlehurst, "On secrecy metrics for physical layer security over quasi-static fading channels," *IEEE Trans. Wireless Commun.*, vol. 15, no. 10, pp. 6913–6924, Oct. 2016.
- [26] L. Fan, X. Lei, N. Yang, T. Q. Duong, and G. K. Karagiannidis, "Secure multiple amplify-and-forward relaying with cochannel interference," *IEEE J. Sel. Top. Signal Process.*, vol. 10, no. 8, pp. 1494–1505, Dec. 2016.
- [27] F. S. Al-Qahtani, C. Zhong, and H. M. Alnuweiri, "Opportunistic relay selection for secrecy enhancement in cooperative networks," *IEEE Trans. Commun.*, vol. 63, no. 5, pp. 1756–1770, May 2015.
- [28] I. S. Gradshteyn and I. M. Ryzhik, *Table of Integrals, Series and Products*, 7th ed. New York: Academic, 2007.
- [29] C. D. Meyer, *Matrix Analysis and Applied Linear Algebra*. SIAM, 2000.
- [30] X. Li and J. Cheng, "Asymptotic error rate analysis of selection combining on generalized correlated Nakagami- m channels," *IEEE Trans. Commun.*, vol. 60, no. 7, pp. 1765–1771, July 2012.
- [31] S. Liu, J. Cheng, and N. C. Beaulieu, "Asymptotic error analysis of diversity schemes on arbitrarily correlated Rayleigh channels," *IEEE Trans. Commun.*, vol. 58, no. 5, pp. 1351–1355, May 2010.
- [32] X. Song, J. Cheng, and N. C. Beaulieu, "Asymptotic analysis of different multibranch diversity receivers with arbitrarily correlated Rician channels," *IEEE Trans. Wireless Commun.*, vol. 13, no. 10, pp. 5676–5689, Oct. 2014.
- [33] N. B. Mehta, S. Kashyap, and A. F. Molisch, "Antenna selection in LTE: From motivation to specification," *IEEE Commun. Mag.*, vol. 50, no. 10, pp. 144–150, Oct. 2012.
- [34] Z. Chen, J. Yuan, and B. Vucetic, "Analysis of transmit antenna selection/maximal-ratio combining in Rayleigh fading channels," *IEEE Trans. Veh. Technol.*, vol. 54, no. 4, pp. 1312–1321, July 2005.
- [35] N. Yang, P. L. Yeoh, M. ElKashlan, R. Schober, and I. B. Collings, "Transmit antenna selection for security enhancement in MIMO wiretap channels," *IEEE Trans. Commun.*, vol. 61, no. 1, pp. 144–154, Jan. 2013.
- [36] F. S. Al-Qahtani, Y. Huang, S. Hessien, R. M. Radaideh, C. Zhong, and H. M. Alnuweiri, "Secrecy analysis of mimo wiretap channels with low-complexity receivers under imperfect channel estimation," *IEEE Trans. Inf. Forensics Security*, vol. 12, no. 2, pp. 257–270, Feb. 2017.
- [37] C. Kundu, S. Ghose, and T. M. N. N. etc, "Effects of CSI knowledge on secrecy of threshold-selection decode-and-forward relaying," *IEEE Access*, vol. 5, pp. 19393–19408, 2017.
- [38] A. Annamalai, G. K. Deora, and C. Tellambura, "Theoretical diversity improvement in GSC(N, L) receiver with nonidentical fading statistics," *IEEE Trans. Commun.*, vol. 53, no. 6, pp. 1027–1035, June 2005.